PYROLYSIS MASS SPECTROMETRIC ANALYSIS OF COPOLYMER OF POLYACRYLONITRILE AND POLYTHIOPHENE

A THESIS SUBMITTED TO
THE GRADUATE SCHOOL OF NATURAL AND APPLIED SCIENCES
OF
MIDDLE EAST TECHNICAL UNIVERSITY

BY

GÜLCAN OGUZ

IN PARTIAL FULFILLMENT OF THE REQUIREMENTS FOR THE DEGREE
OF
MASTER OF SCIENCES
IN
POLYMER SCIENCE AND TECHNOLOGY

JUNE 2004

Approval of the Graduate School of Natural and Applied Sciences

Prof.Dr. Canan Özgen
Director

I certify that thesis satisfies all the requirements as a thesis for the degree of Master of Sciences.

Prof.Dr. Ali Usanmaz
Head of the Department

This is to certify that we have read this thesis and that in our opinion it if fully adequate, in scope and quality, as a thesis for the degree of Master of Sciences.

Prof.Dr. Ahmet M.Önal Co-Supervisor	Prof.Dr. Jale Hacaloglu Supervisor

Examining Committe Members

Prof.Dr. Kemal Alyürük	(METU,CHEM)	
Prof.Dr. Jale Hacaloglu	(METU,CHEM)	
Prof.Dr. Ahmet M.Önal	(METU,CHEM)	
Prof.Dr. Zuhal Küçükyavuz	(METU,CHEM)	
Prof.Dr. Bekir Salih	(Hacettepe University,CHEM)	

I hereby declare that all information in this document has been obtained and presented in accordance with academic rules and ethical conduct. I also declare that, as required by these rules and conduct, I have fully cited and referenced all material and results that are not original to this work.

Name, Last name: Gülcan Oguz

Signature :

ABSTRACT

PYROLYSIS MASS SPECTROMETRIC ANAYSIS OF COPOLYMER OF POLYACRYLONITRILE AND POLYTHIOPHENE

Oguz, Gülcan
M.Sc., Polymer Science and Technology
Supervisor : Prof.Dr.Jale Hacaloglu
Co-Supervisor: Prof.Dr.Ahmet M.Önal

June 2004, 70 pages

In the first part of this work, the structural and thermal characteristics of polyacrylonitrile, polyacrylonitrile films treated under the electrolysis conditions in the absence of thiophene, polythiophene and the mechanical mixture and a conducting copolymer of polyacrylonitrile/polythiophene have been studied by pyrolysis mass spectrometry technique.

The thermal degradation of polyacrylonitrile occurs in three steps; evolution of HCN, monomer, low molecular weight oligomers due to random chain cleavages are followed by cyclization and dehydrogenation reactions yielding crosslinked and unsaturated segments. Pyrolysis of the treated polyacrylonitrile films indicated decrease in the yields of monomer and oligomers, and increase in the amount of products stabilized by cyclization reactions were detected. Polythiophene degrades in two steps; the loss of the dopant and degradation of polymer backbone.

The evolution profiles of polythiophene based products from polythiophene/polyacrylonitrile showed nearly identical trends with those recorded

during the pyrolysis of pure polythiophene. However, evolution of HCN and the degradation products due to the homolytic cleavages of the polymer backbone continued through out the pyrolysis indicating a significant increase in their production. Furthermore, the yield of thermal degradation products associated with decomposition of the unsaturated cyclic imine segments decreased. A careful analysis of the data pointed out presence of mixed dimers confirming copolymer formation.

In the second part of this work, a poly(acrylonitrile-co-butadiene) sample involving monomer units having quite similar molecular weights have been analyzed to investigate the limits of the pyrolysis mass spectrometry technique. Pyrolysis of aged poly(acrylonitrile-co-butadiene) indicated oxidative degradation of the sample.

Keywords: conducting copolymer, polyacrylonitrile, polythiophene, polybutadiene, direct pyrolysis mass spectrometry

ÖZ

POLIAKRILONITRIL VE POLITIYOFEN KOPOLIMERININ PIROLIZ KÜTLE SPEKTROMETRESI ILE ANALIZI

Oguz, Gülcan
Yüksek Lisans, Polimer Bilimi ve Teknolojisi
Tez Yöneticisi : Prof.Dr.Jale Hacaloglu
Ortak Tez Yöneticisi: Prof.Dr.Ahmet M.Önal

Haziran 2004, 70 sayfa

Çalismanin ilk asamasinda, poliakrilonitril, poliakrilonitril film örnekleri, politiyofen ve poliakrilonitril/politiyofen iletken kopolimeri ve mekanik karisiminin isil davranimi, isil bozunum ürünleri ve isil bozunum mekanizmasi direkt piroliz kütle spektrometre teknigi kullanilarak incelendi.

Piroliz analiz sonuçlari, poliakrilonitrilin isil bozunumunun üç asamada gerçeklestigini göstermistir. Ilk asamada, polimer zincirinde rastgele kopmalarin meydana geldigi ve HCN, monomer ve düsük molekül agirlikli oligomerlerin olustugu gözlenmistir. Ikinci asamada polimer zincirinde doymamis ve çapraz baglar olusmaktadir. Sicakligin artmasi durumunda ise doymamis baglarin arttigi ve tüm polimer zincirinde yayginlastigi görülmüstür. Poliakrilonitril film örneklerinin piroliz analiz sonuçlarina göre, monomer ve oligomer verimlerinde azalma görülmekte ve polimer zincirinde çapraz baglarda bir artistan dolayi daha kararli bir yapi meydana geldigi görülmektedir. Politiyofenin bozunmasi iki asamada olmaktadir. Ilk asamada katki bozunumu ikinci asamada ise polimer bozunumu gerçeklesmektedir.

Poliakrilonitril/politiyofen kopolimerinin detayli analiz sonucu, kopolimerden kaynaklanan politiyofenin saf politiyofen ile benzer davranisi gösterdigi anlasilmistir. Fakat, poliakrilonitrilden kaynaklanan HCN'in iyon veriminde bir artis gözlenmektedir. Ayrica, doymamis halkali yapidaki imin segmentlerinin bozunmasindan dolayi olusan isil bozunum ürünlerinin iyon verimlerinde azalma olmaktadir. Detayli piroliz analiz sonuçlari, mix-dimerlerin varligindan dolayi kopolimerlesmenin gerçeklestigi seklinde yorumlanmaktadir.

Çalismanin ikinci asamasinda, monomer birimleri yaklasik ayni molekül agirligina sahip olan poliakrilonitril/polibutadien kopolimeri, direkt piroliz kütle spektrometre teknigi kullanilarak incelendi. Oksijene maruz kalan poliakrilonitril/polibutadien kopolimerinin piroliz analizi sonucu, maddenin oksitlenmeyle bozundugunu göstermistir.

Anahtar kelimeler: iletken kopolimer, poliakrilonitril, politiyofen, polibutadien, direkt piroliz kütle spektrometresi

TO MY LOVELY FAMILY

ACKNOWLEDGEMENTS

I express my appreciation to Prof.Dr.Jale Hacaloglu and Prof.Dr.Ahmet M. Önal for their guidance and encouragement throughout this work. I also want to thank to them for their great patience during my studies.

I would like to thank to Birim Ileri and Hürmüs Refiker for their moral support and help.

I also want to thank to Atilla Cihaner, Seha Tirkes and Mustafa Tabar for their help.

TABLE OF CONTENTS

LIST OF TABLES

TABLE

LIST OF FIGURES

FIGURE

CHAPTER I

INTRODUCTION

I.1. Conducting Polymers

Conducting polymers, also sometimes called conjugated conducting polymers or organic polymeric conductors, are materials consisting of polymeric molecules, which have high electrical conductivity. Electron conjugation along the backbone of the polymer chain is one of the criteria for a polymer to behave as an electrical conductor. Delocalization of electrons occurs through the interaction of π - electrons in a highly conjugated chain or by a similar interaction of π - electrons with nonbonded electrons of the heteroatoms such as sulphur and nitrogen present in the backbone. The conductivity of conducting polymers is achieved through chemical or electrochemical oxidation or reduction by a number of simple anionic or cationic species called dopants. The polymeric backbone of these materials needs to be oxidized or reduced to introduce charge centers before conductivity is observed and the oxidation or reduction is performed by anions or cations [1].

Until 1970, many conducting polymers were known as insulators before their conductivity and other properties of interest were discovered. The modern era of conducting polymers (CPs) began when Heeger and MacDiarmid discovered high conductivity in polyacetylene ($(CH)_x$), synthesized by Shirakawa's method [2]. Polyacetylene became conducting after oxidation by suitable reagents [3].

An important step in the development of conjugated poly(heterocycles) occurred when highly conducting and homogeneous free standing films of polypyrrole produced by oxidative electropolymerization of pyrrole. Then, the electrochemical polymerization has been rapidly extended to other aromatic compounds such as thiophene, furan, indole, carbazole, azulene, pyrene, and fluorene, which have π - electrons and heteroatom.

Although conducting polymers have some advantages such as low density and easy processibility, they do not have good environmental and thermal stability. Therefore, in order to improve their properties, composites or copolymers of conducting polymers are obtained [4-7].

I.1.2. Electrical Conduction

The materials may be classified into three categories according to their conductivity properties as insulators, semiconductors and conductors.

Figure I.1 shows the energy diagram for a metal, a semiconductor and an insulator. The energy difference between the valance band (the highest occupied band) and the conduction band (the lowest unoccupied band) is called band gap (E_g). The size of this gap determines the conductivity of the materials. In metals, high conductivity is due to partially occupied valance band or overlapping between valance and conduction bands. In a semiconductor, E_g is narrow and the movement of electrons from the valance band to the conduction band provides the conduction. On the other hand, an insulator has a wider E_g. Therefore the electrons cannot be transferred from the valance band to the conduction band under normal conditions.

I.1.3. Doping

Conductive organic polymers are generally insulator or semi-conductors in their undoped state but they can be made as conductive as metals when they are subjected to a doping process [8-9].

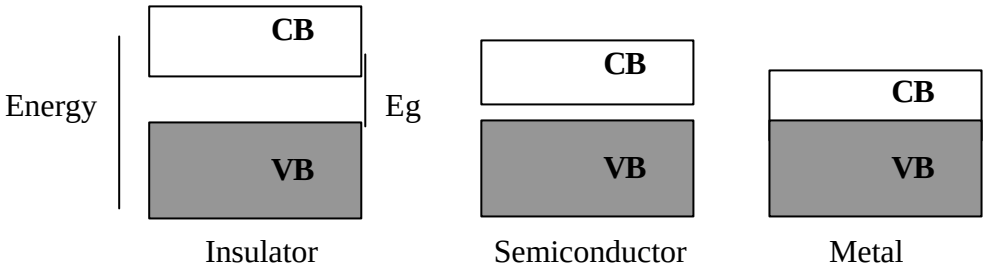

Figure I. 1 Schematic diagram of the band structure of a metal, a semiconductor and an insulator. VB and CB represents the valance band and the conduction band respectively. Black region states the occupied electronic state and white region represents the unoccupied electronic state

Oxidation of a conjugated polymer, which is essentially removal of electrons from the valance band, introduces charge centers on the polymer. These charge centers are in general strongly delocalized over several monomer units in the polymer. A charge can also be donated to the conduction band of the conjugated polymer which causes reduction of the polymer, producing charge centers again.

The chemical oxidation of the conducting polymers by anions or reduction by cations is called doping [10] and the associated anions or cations are called dopants.

The doping of a conducting polymer can be accomplished chemically [3] or electrochemically [11-12]. Chemical doping is achieved by exposure to a solution or vapor of the dopant. In electrochemical doping, potential is applied to the conducting polymer in solution. When a positive potantial is applied to a conjugated polymer, the dopant anions move from the solution into the conducting polymer towards the delocalized charge sites on the conjugated polymer This is called as anionic doping or p-type doping. If a negative potential is applied to a conjugated polymer, cations move from the solution into the polymer. This is termed as cationic or n-type doping [13-14].

The initial insulating state of the conjugated polymer can be achieved by a reverse process, called as dedoping. In the dedoping process, the dopant physically moves out of the conducting polymer lattice.

I.1.4. Electrochemistry of Conducting Polymers

Although conducting polymers can also be prepared chemically [3], the most convenient and most widely used method for synthesis of conducting polyheterocycles is the electrochemical anodic oxidation [2, 15-16]. It is important that the doping process is analysed by electrochemical polymerization.

Electrochemical polymerization of conducting polymers have several advantages, such as:

- Polymer films are directly formed at the electrode surface,
- Uniform coatings can be more easily obtained,
- The thickness of the film can be controlled,
- The process takes place in the absance of any extraneous reagents,
- Characterization can be performed also by electrochemical techniques.

I.1.5. Effects of Electrosynthesis Conditions on Electrochemical Polymerization

The electrochemical polymerization of five membered heterocycles depends on many experimental variables such as the solvent, the concentration of the reagents, the temperature, the cell geometry, the nature and the shape of the electrodes, and the applied electrical conditions. Electrosynthesis conditions determine the structure and properties of the resulting polymer [17].

The nature the dopant and the solvent are the two important parameters for the electrochemical polymerization of conducting polymers. If the electrochemical polymerization reaction proceeds via radical cation intermediates, then the nucleophilic character of the solvent and the electrolyte imposes certain restrictions on their choice.

The solvent must have a high dielectric constant to provide the ionic conductivity of the electrolytic medium and a good electrochemical resistance against decomposition

at the oxidation or reduction potential of the monomer. Therefore, most of the conductive polymers synthesised electrochemically by oxidation have been prepared in anhydrous aprotic solvents of high dielectric constant and low nucleophilicity such as acetonitrile, benzonitrile, nitrobenzene and propylene carbonate. Several works have shown that the presence of traces of water in the synthesis medium has harmful effect on the electropolymerization reaction and on the conductivity of the polymer formed.

The choice of the supporting electrolyte depends on the solubility, the degree of dissociaton and the nucleophilicity. Quarternary ammonium salts of the type R_4NX (where R=alkyl or aryl radical and X=Cl, Br^-, ClO_4^-, BF_4^-, PF_6^-, $CF_3SO_3^-$ or $CH_3C_6H_4SO_3^-$) are soluble in aprotic solvents and are highly dissociated in them. Therefore, these salts are commonly used as the supporting electrolytes in the electrochemical polymerization of the conducting polymers.

The concentration of the monomer is another important parameter that affects the conductivity of the polymer. Under the same electrochemical conditions, high monomer concentrations produce loose and poorly conducting films containing significant amounts of soluble oligomers. Low monomer concentrations improve both the cohesion of the films and the conductivity.

The temperature of electropolymerization has been reported to affect the extent of the conjugated system and electrochemical properties. When the temperature increased, decrease in conductivity was observed. Temperature promotes termination step and therefore oligomers with smaller conjugation lengths are formed instead of high molecular weight chains being deposited as an insoluble polymer on the electrode surface [18].

In electrochemical polymerization, a standard three electrode system composed of a working electrode, a counter electrode and a reference electrode, is generally used. If the polymeric films are deposited by an oxidative process, it is necessary that the electrode should not oxidize with the monomer. For this reason, inert electrodes like Pt, Au, SnO_2 substrates, ITO and stainless substrates are used as working electrode.

A metallic foil of Pt, Au or Ni is used for a counter electrode and a SCE and $Ag/AgCl^{+}$ electrodes can be used as a reference electrode.

I.2. Polythiophene

Polythiophene (PTh) is one of the most frequently used conducting polymer in commercial applications due to its long term stability of its conductivity and the possibility of forming copolymers or composites with optimal mechanical properties. Therefore, it has a number of advantages compared to other polyheterocyclics, for example a) it is possible to prepare conducting polymers from a wide range of β-substituted thiophenes, b) the extent of oxidative doping can be very high, c) it is possible to produce conducting polymer by reduction, as well as oxidation of the neutral polymer [19].

PTh can be synthesized both chemically and electrochemically. Chemical synthesis has an advantages of mass production at low cost. However, in chemical synthesis products are in powder form having low conductivity, whereas in electrochemical polymerization freestanding films having high conductivity can be obtained. In addition to high environmental stability of its doped and undoped states, it has controllable electrochemical behavior, electroactivity and conductivity.

I.2.1. Mechanism of Electropolymerization of Polythiophene

The electropolymerization of aromatic compounds occurs via an unique mechanism which has been more extensively analyzed using pyrrole as a model compound.

The electropolymerization reaction proceeds with electrochemical stochiometry within values in the range of 2.07-2.5 Faradays/mol. The oxidation of monomer requires 2 electrons/molecule while the excess of charge corresponds to the reversible oxidation or doping of the polymer. The polymerization is initiated from 2 and 5 positions of thiophene monomer [20,21].

Imanishi proposed a two step mechanism for the polymerization of these aromatic compounds [8]. The proposed mechanism of electropolymerization of thiophene by radical coupling is represented in Figure I.2. The first electrochemical step consists the oxidation of the monomer to its radical cation. Since the electron transfer reaction is much faster than the diffusion of the monomer from the bulk of the solution, a high concentration of radicals is continuously maintained near the electrode surface. The second step involves the coupling of two radicals to produce a dihydro dimer cation which leads to a dimer after the loss of two protons and the rearomatization. Due to the applied potential, the dimer, which is more easily oxidized than the monomer, occurs in its radical form and undergoes a further coupling with a monomeric radical. Electropolymerization proceeds through successive electrochemical and chemical steps until the oligomer becomes insoluble in the electrolytic medium and precipitates onto the electrode surface.

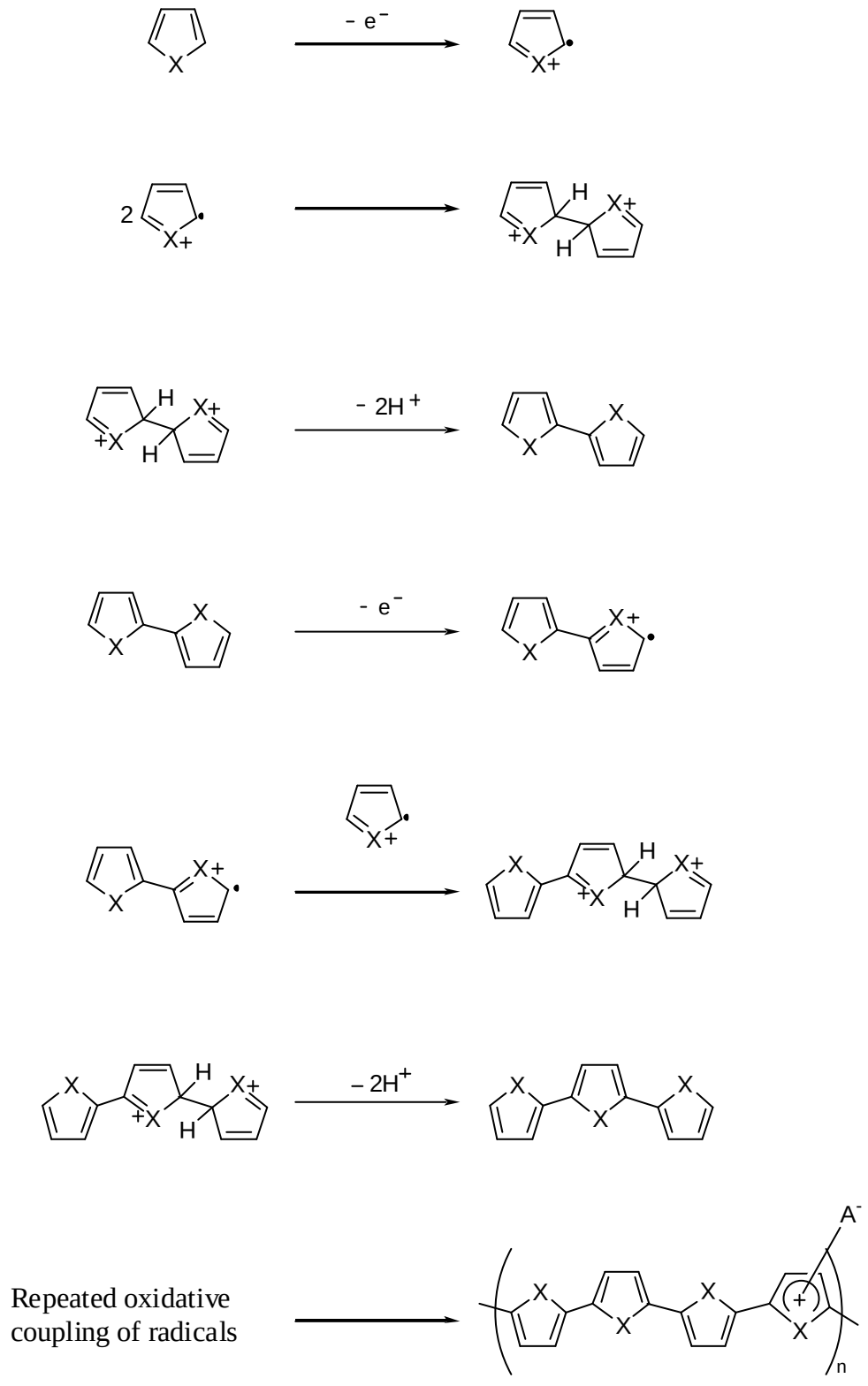

Figure I. 2 The mechanism of electropolymerization of thiophene

I.2.2. Structure of Polythiophene

In PTh, the monomeric units are coupled through the 2 and 5 positions with a degree of polymerization that varies widely but is relatively high [20]. The ideal structure of PTh is shown below:

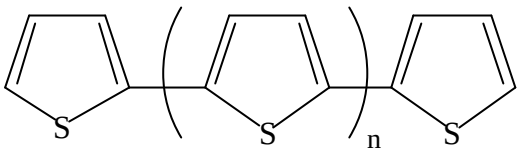

Further support for the coupling of thiophene through 2-5 positions comes from solid state nuclear magnetic resonance (NMR) [22] and infrared (IR) spectroscopy experiments [23].

Moreover, it has been suggested that PTh has two mesomeric structures as aromatic and quinoid structure [24]. Among the two fundamental structures, the aromatic structure corresponds to the undoped (neutral form) and quinoid structure corresponds to the doped state (oxidized form). These two forms are not energetically equivalent, the quinoidal form has higher energy.

Aromatic form

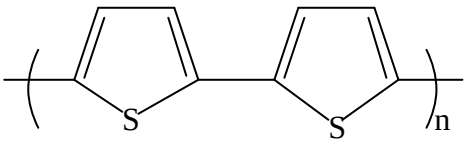

Quinoid form

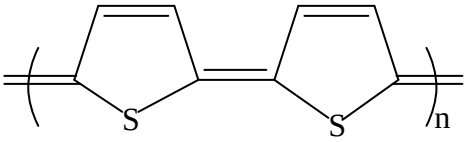

I.2.3. Thermal Degradation of Polythiophene

Degradation studies of electrochemically synthesized BF_4^-doped PTh and ClO_4^- doped PTh in air have shown that the rate of degradation is dependent on the counter ion [25, 26]. Morever, another study has shown that the rate of degradation is more rapid for ClO_4^- and less rapid for AsF_6^-.

The PTh films were found to be thermally stable to heating at 80 ^{0}C for several hours but the thermal degradation of polythiophene at longer periods at this temperature was confirmed by the decrease in conductivity. The conductivity decreased substantially upon heating to temperature above 70 ^{0}C for ClO_4^- and AsF_6^- doped polythiophenes.

TGA analysis showed that polythiophene is stable up to around 500 ^{0}C, above this temperature it rapidly degrades away completely. According to TGA and IR results, the main weight loss appears in the wide range of 400 and 600 ^{0}C for both the doped and dedoped samples. No appriciable change was observed for the fractions of the elements in these temperature ranges [27, 28].

FTIR studies showed that the degradation of BF_4^-doped PTh aged at different temperatures involves two steps. Step one seems to correspond to the loss of the counterion by some complex chemical reaction but without any loss of conjugation. Step two corresponds to the oxidative reactions of the polymer backbone producing segments of various conjugation lengths. When aged at 80 ^{0}C, an increase to a maximum then a continuous decay in the intensity of the band associated with 2,5 linkages was observed with an induction period of about five days. A continuos fall in the intensities of the dopant induced band were also observed [29]. Recent studies on pyrolysis of BF_4^- and PF_6^- doped PTh supported these results.

I.2.4. Conducting Copolymers of Polythiophene

The π-electron system along the polymer backbone leads to rigidity and crosslinking. The crosslinking in the conducting polymer chain makes the polymer insoluble and therefore, poorly processable [2,30-37]. In order to improve mechanical characteristics, several methods have been suggested. A convenient method to improve their processibility is the synthesis of block and graft copolymers containing conventional and conducting sequences, where conventional sequences increase the solubility of the resultant block and graft copolymer. Blending conducting polymer with thermoplastic polymers is another attempt to increase their processibility. The composites and graft copolymers are commonly synthesized by coating of the insulating polymer on an electrode, which is then used as the anode for the electropolymerization of the conducting component.

There have been several studies on preparation of composite and copolymers of polythiophene. The composites of polythiophene were synthesized by growing a thin coating of the insulating polymer, such as polyvinylchloride, poly(bisphenol A carbonate), polystyrene and polyamide, on an electrode [2,38]. Graft and block copolymers of polystyrene and polythiophene were also synthesized. Of course, the copolymers of thiophene are much more preferable than composites of polythiophene due to their homogeneity, well defined structure and good mechanical properties.

I.2.5. Applications of Polythiophene

Polythiophene is used for several technological applications. These applications can be divided into three main groups according to the

a) electrical properties of the doped conducting state
The first domain of application contains antistatics, electromagnetic interference (EMI) shielding and gas sensors.

b) electronic properties of the neutral semiconducting state

Various types of electronic devices such as, photovoltaic cell, photoelectrochemical cells and photorechargeable devices are based on undoped state of polythiophene. Also, Schottky barriers and field effect transistors (FET) involve polythiophene films.

c) electrochemical reversibility of the transition between the doped and undoped state

The considerable spectral changes in the visible region associated to the doping/undoping process of polythiophene have led to several proposals of electrooptical systems such as display devices and electrochromic windows.

I.3. Polyacrylonitrile

Polyacrylonitrile (PAN) is a vinylic homopolymer with the repeating unit –(CH_2-CHCN)-, usually produced in the atactic form. It is mainly used in clothing and soft furnishing, but PAN is also an important carbon fiber precursor [39].

I.3.1. Thermal Degradation of Polyacrylonitrile

Grassie and McGuchan studied the thermal degradation of polyacrylonitrile by thermal volatilization analysis (TVA) and found that ammonia and hydrogen cyanide were the main products of degradation [40, 41].

Coleman and co-workers suggested that the degradation began as early as 160 ^{0}C under vacuum as evidenced by the disappearance of the 2240 cm^{-1} band for the nitrile. Also, during pyrolysis, the structure of polyacrylonitrile is changed through two heating stages. First, a single conjugated structure of imine moieties is formed by polymerization of pending CN groups. This stage is reported to occur at 200-300 ^{0}C, also in the presence of air. The double conjugated ladder structure is achieved by heating in vacuum or under N_2 at temperatures > 300 ^{0}C. The pyrolysis mechanism of polyacrylonitrile is shown in Figure I.3 [42]. When the infrared spectra of heat treated films, in the temperature range 200-600 ^{0}C in vacuum, was examined, it has

been determined that the pyrolysis process occurred in three steps: cyclization, de-hydrogenation and de-nitrogenation [43].

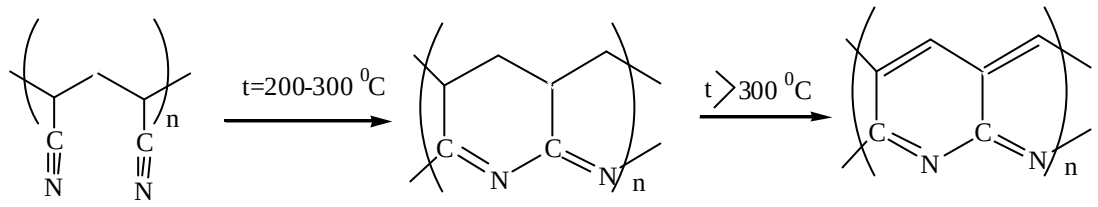

Figure I. 3 The pyrolysis mechanism of polyacrylonitrile

The chemical changes occurring in the thermal degradation of PAN is essentially a twin process in which a) structure stabilization leads to the formation of cyclic product (residue) as a result of oligomerization of nitrile groups and b) homolytic cleavage of the backbone polymer chain yields gaseous and volatile products. The decomposition process can produce as much as 40% of gaseous products (% wt of PAN).

1.4. Polybutadiene

Polybutadiene (PB) with the repeating unit $-(CH_2\text{-}CH{=}CH\text{-}CH_2)_n-$ is one of the first types of synthetic elastomers or rubbers to be invented. It is amorphous and its glass transition temperature is -106 ^{0}C. Therefore, tires, belts, hoses, gaskets and other automobile parts are made from polyubutadiene, because it stands up to cold temperatures better than other elastomers [44].

1.4.1. Thermal Degradation of Polybutadiene

The DTA thermogram being obtained by the pyrolysis of PB in nitrogen atmosphere shows that there are two exotherm and two endoterm peaks at 383 ^{0}C, 546 ^{0}C and 440 ^{0}C, 512 ^{0}C, respectively. Combining results of FT-IR for the residues of PB, it is concluded that the exotherm at 390 ^{0}C and the endotherm at 450 ^{0}C represent cyclization and depolymerization, respectively. At 450 ^{0}C, the major pyrolysis

process is depolymerization and xylene is obtained in significant yield. At higher temperatures (600 ^{0}C), the lower molecular products predominate due to decomposition [44, 45].

In DSC curve of PB, three features are observed, such as cis-trans isomerization near 220 ^{0}C, cyclization at about 380 ^{0}C, and the degradation endotherm at about 480 ^{0}C [45].

The pyrolysis-GC results indicates that the major pyrolysis products of PB are butadiene (C_4H_6), cyclopentene (C_5H_8), cyclohexene (C_6H_{10}), 1,4, cycloheptadiene (C_7H_{10}) and 4-vinylcyclohexene (C_8H_{12}) [46].

I.5 Pyrolysis Mass Spectrometry

Pyrolysis is the thermal degradation of a complex material in an inert atmosphere or vacuum. It causes molecules to cleave at their weakest points to produce smaller, volatile fragments called pyrolysate [47].

Pyrolysis-mass spectrometry (Py-MS) is a very fast and sensitive fingerprinting technique. In this method, the sample is placed in high vacuum and heated under controlled conditions. The organic materials undergoes rapid decomposition and the low molecular weight products enter into a mass spectrometry device, where the pyrolysate is quantified [48].

Since pyrolysis mass spectrometry techniques are carried out under high vacuum conditions, the possibility of secondary reactions is minimized [49].

Pyrolysis mass spectrometry techniques can be used to determine not only the thermal behavior and the decomposition products but also to investigate the structure of the polymers [50-52].

Among the various pyrolysis mass spectrometry techniques, direct pyrolysis mass spectrometry technique allows the thermal decomposition products of the polymer sample to be generated directly in the ion source of the mass spectrometer.Thus, the evolving products are ionized and continuously detected by repetitive mass scans almost simultaneously with their formation. Since pyrolysis is accomplished under high vacuum, the thermal degradation fragments are removed from the hot zone, thus molecular collisions have low probability and the generation of secondary reactions is reduced [53]. It is a simple and quick method for structural and thermal characterization of polymers [52,54].

I.6. Aim of The Study

The objectives of this study are:

- to prepare conducting copolymer of polyacrylonitrile/polythiophene (PAN/PTh) by electrochemical polymerization of thiophene on a polyacrylonitrile coated electrode

- the structural and the thermal characterization of BF_4^- doped PAN/PTh by direct insertion probe pyrolysis mass spectrometry

- to investigate the effects of each component of the copolymer on structural and thermal characteristics

- to investigate limitations of direct insertion probe mass spectrometry technique for characterization of a copolymer involving components having repeating units with similar molecular weights.

CHAPTER II

EXPERIMENTAL

II.1. Materials

Thiophene (Th) and acetonitrile (CH_3CN) were purified by distillation prior to electrolysis and stored at 4 ^{0}C. Tetrabutylammonium tetrafluoroborate (TBAFB) was used after purification by recrystallization. Dimethylsulfoxide (DMSO) (Merck), polyacrylonitrile (PAN) (Sigma-Aldrich), trans 1,4 polybutadiene (PB) and poly(acrylonitrile-co-butadiene) (PANB) (Sigma-Aldrich) were used without further purification.

II.2. Instrumentation

II.2.1. Potentiostat

A HEKA IEE 488 potentiostat was used to provide the constant potential between the working and reference electrodes during the electrolysis.

II.2.2. Electrolysis Cell

The electrochemical polymerization reactions were carried out in a three compartment cell with three electrode configuration in acetonitrile. Platinum plates (1.5 cm^2) were used as working and counter electrodes and Ag/Ag^+ electrode was used as the reference electrode. Tetrabutylammonium tetrafluoroborate was used as the supproting electrolyte.

II.3. Mass Spectrometer

Direct insertion probe pyrolysis mass spectrometry (DIP-MS) system consists of a 5973 HP quadrupole mass spectrometer coupled to a JHP SIS direct insertion probe. This system provides fast scanning, self-tuning of experimental parameters and wide mass range. Mass spectra of the products was recorded at a scan rate of 2 scan/s in the mass range of 10-800 amu.

The major components of the mass spectrometer are vacuum system, sample inlet, ion source, mass filter, detector and the data system (Figure II.1).

II.3.1. Vacuum System

The vacuum system creates the high vacuum (low pressure) required for the mass spectrometer to operate so that it makes it possible for ions generated by electron impact in the ion source to move from the ion source to the quadrupole analyzer where they are separated according to their mass to charge (m/z) ratios and then to the detector without collisions with other ions and molecules. A high vacuum is obtained by diffusion and rotary vane pumps.

II.3.2. Sample Inlet

The Direct Insertion Probe Pyrolysis technique is employed by a SIS direct inlet probe. The heating rate can be controlled by a thermocouple attached to the probe tip inside the probe rod and the probe tip is in direct contact with flared glass sample vials that can be inserted and removed from the direct probe inlet easily.

The heating rates are programmed with the use of probe software. Generally, ramping heating is applied. Direct pyrolysis experiments were performed by applying a programme which allows a heating rate of 10 ^{0}C/min. In each experiment, the temperature was increased up to 445 ^{0}C, (the maximum attainable temperature) and kept constant for an additional 10 minutes at 445 ^{0}C. Each set of analysis involves 5400 mass spectra.

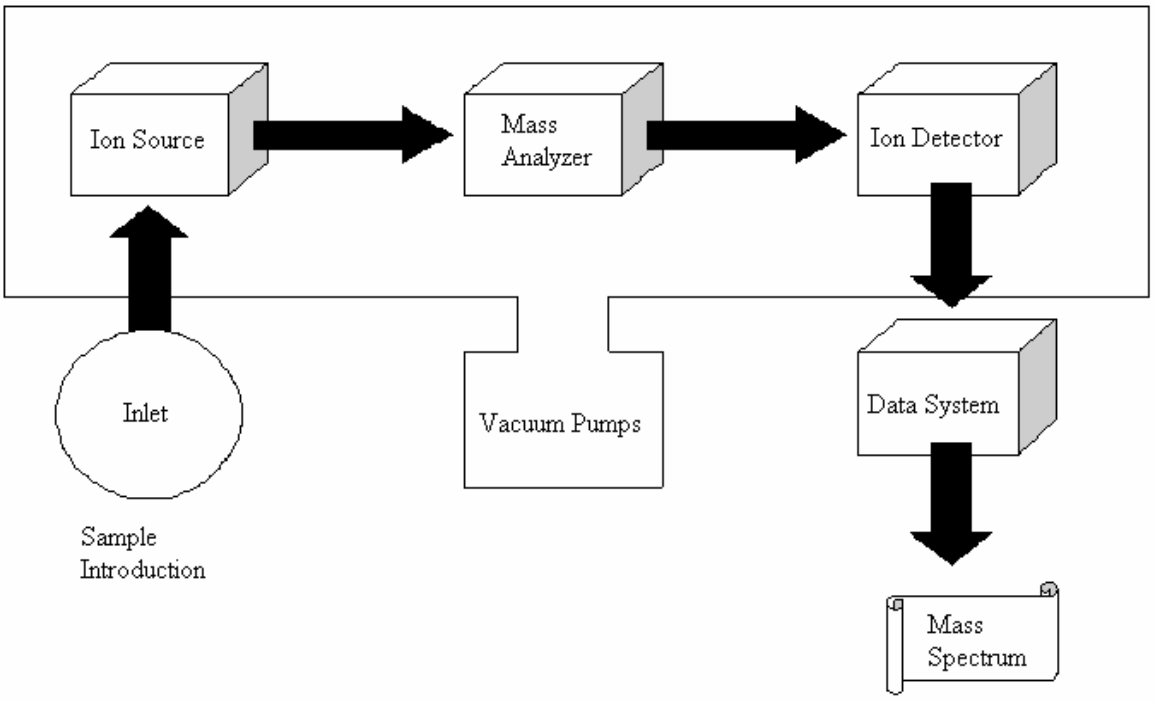

Figure II. 1 Block diagram of mass spectrometer

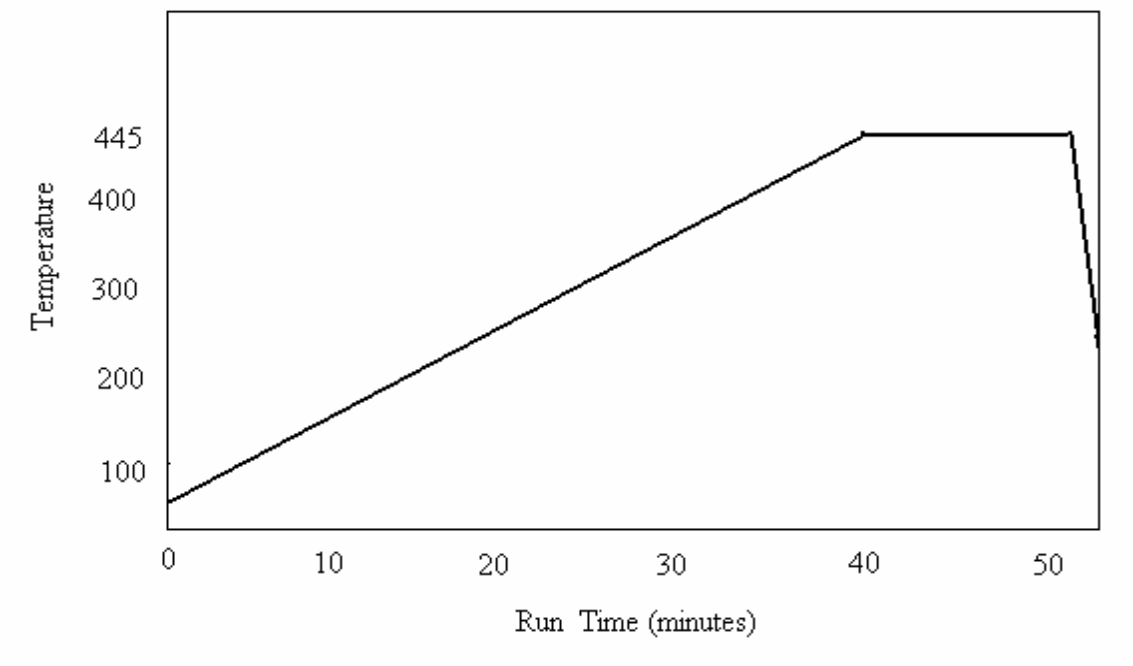

Figure II. 2 Path of Ramp Heating in Direct Insertion Probe

II.3.3. Ion Source

Sample molecules enter the ion source from the sample inlet. Before the ion source, the sample molecules must be converted into the pyrolyzed form. In the ion source, ionization and fragmentation of the molecules are occurred.

The ion source operates by electron impact ionization (EI). In electron impact ionization, the sample molecules are bombarded with high energy electrons, and then positive ions are produced. Because EI produces a large number of fragment ions, it is a hard ionization method and useful for structural information.

In the present study, in general the ionization energy used was 70 eV. Experiments were also repeated decreasing ionization energy (20 eV) to minimize secondary dissociation of the thermal decomposition products during ionization.

II.3.4. Mass Filter

The mass filter separates ions according to their mass to charge ratio (m/z). At a given RF to DC ratio, only ions of a selected mass to charge ratio can pass through the mass filter to the detector. The analyzer is a quadrupole mass filter and amplifies.

II.3.5. Detector

The detector in the spectrometer is a high energy conversion dynode (HED) coupled to an electron multiplier (EM). The detector is located at the exit end of the quadrupole mass filter. It recevies the ions that have passed through the mass filter.

II.4. Synthesis

II.4.1. Preparation of Polyacrylonitrile Films

Insulating polymer films were dip-coated from 4.1 % PAN solution which had been prepared by dissolving polyacrylonitrile in DMSO. In order to investigate the effects

of CH_3CN/TBABF solvent-electrolyte system and the applied potential of 1.9 V on PAN film samples were left in acetonitrile with or without the application of 1.9 V potential (0.1 mA current) for variable time periods.

II.4.2. Electrochemical Synthesis of Copolymer of Polyacrylonitrile-Polythiophene

Electropolymerization of thiophene was performed in a cell having a three-electrode system at a constant potential of 1.9 V. The electrolysis cell was equipped with Pt foils (1.5 cm^2) as working and counter electrodes, and Ag/Ag^+ electrode as the reference electrode. 0.05 M CH_3CN/TBAFB solvent-electrolyte system was used. 480 µL pure thiophene was placed into the cell and the polymerization potential was adjusted to +1.9 V. At the end of the electrolysis, a black polymer film formed on the electrode. Polymer films obtained were washed with acetonitrile in order to remove TBAFB crsytals and any trace of monomers and dimers adsorbed on the films and then dried at 30^0C under vacuum. The composites of PAN/PTh were prepared under the same conditions. Yet, electrochemical oxidation of thiophene was achieved by using PAN coated Pt electrode as a working electrode.

CHAPTER III

RESULTS AND DISCUSSION

In general, pyrolysis mass spectra of polymers are quite complicated as thermal degradation products of the polymer further dissociate during the ionization in the mass spectrometer. Pyrolysis mass spectra of copolymers are even more complicated as peaks due to both components appear in the spectra. In order to investigate the structural and the thermal characteristics of electrochemically prepared BF_4^- doped polythiophene onto a poly(acrylonitrile) coated electrode pyrolysis mass spectrometry analyses of the related components, namely poly(acrylonitrile), polythiophene and the mechanical mixtures of polyacrylonitrile and polythiophene have also been performed and discussed. Similarly, in order to investigate the limits of the pyrolysis analyses technique for a copolymer involving similar components not only poly(acrylonitrile-co-butadiene) but also polybutadiene and the mechanical mixtures of PB and PAN have been carried out.

III.1.Polyacrylonitrile

Direct insertion probe pyrolysis mass spectrometry (DIP-MS) technique was used to perform the thermal and the structural characterization of commercial polyacrylonitrile (PAN) and PAN films treated under different conditions.

III.1.1. PAN Powder

The total ion current (TIC) curve that is the variation of total ion intensity as a function of temperature, of PAN is given in Figure III.1. Two peaks with maxima at 310 and 370 ^{0}C and a shoulder at 440 ^{0}C can be seen in the TIC curve. Moreover, the mass spectra recorded at these temperatures are also included in Figure III.1.

Analyses of 70 eV pyrolysis mass spectra at 310 ^{0}C showed that the peaks due to CH_2CH_2CN (m/z=54 Da), CH (CH_2CHCN) (m/z=66 Da), $(CH_2CHCN)_2H$ (m/z=107 Da) and $CH(CH_2CHCN)_2$ (m/z=119 Da) were the most intense ones. Furthermore, the monomer and the oligomer peaks up to six monomer units were recorded. The data obtained at this temperature indicated that random chain cleavages were occurred in the polymer backbone.

At higher temperatures, it has been known that crosslinked and unsaturated bonds are occurred in the polymer backbone. The mass spectrum recorded at 370 ^{0}C is quite similar to that recorded at 310 ^{0}C and involves the same fragment peaks. The peaks due to CH_2CH_2CN (m/z=54 Da), $CH(CH_2CHCN)$ (m/z=66 Da), $(CH_2CHCN)_2H$ (m/z=107 Da) and $CH(CH_2CHCN)_2$ (m/z=119 Da) are again the most abundant. Furthermore, the monomer and the low molecular weight oligomer peaks are also present. However, monomer peak intensity is higher than that of the dimer in the pyrolysis mass spectra recorded around 370 ^{0}C contrary to the ones recorded around 310 ^{0}C.

The mass spectra recorded at the final stages of pyrolysis are significantly different. A detailed analyses of the thermal degradation products indicated that the polymer backbone possessed unsaturated bonds at elevated temperatures. It can be concluded that unsaturation increased along the polymer backbone as the temperature increased. Actually, it has been known that at higher temperatures polyacrylonitrile is used to make carbon fiber and graphite [55].

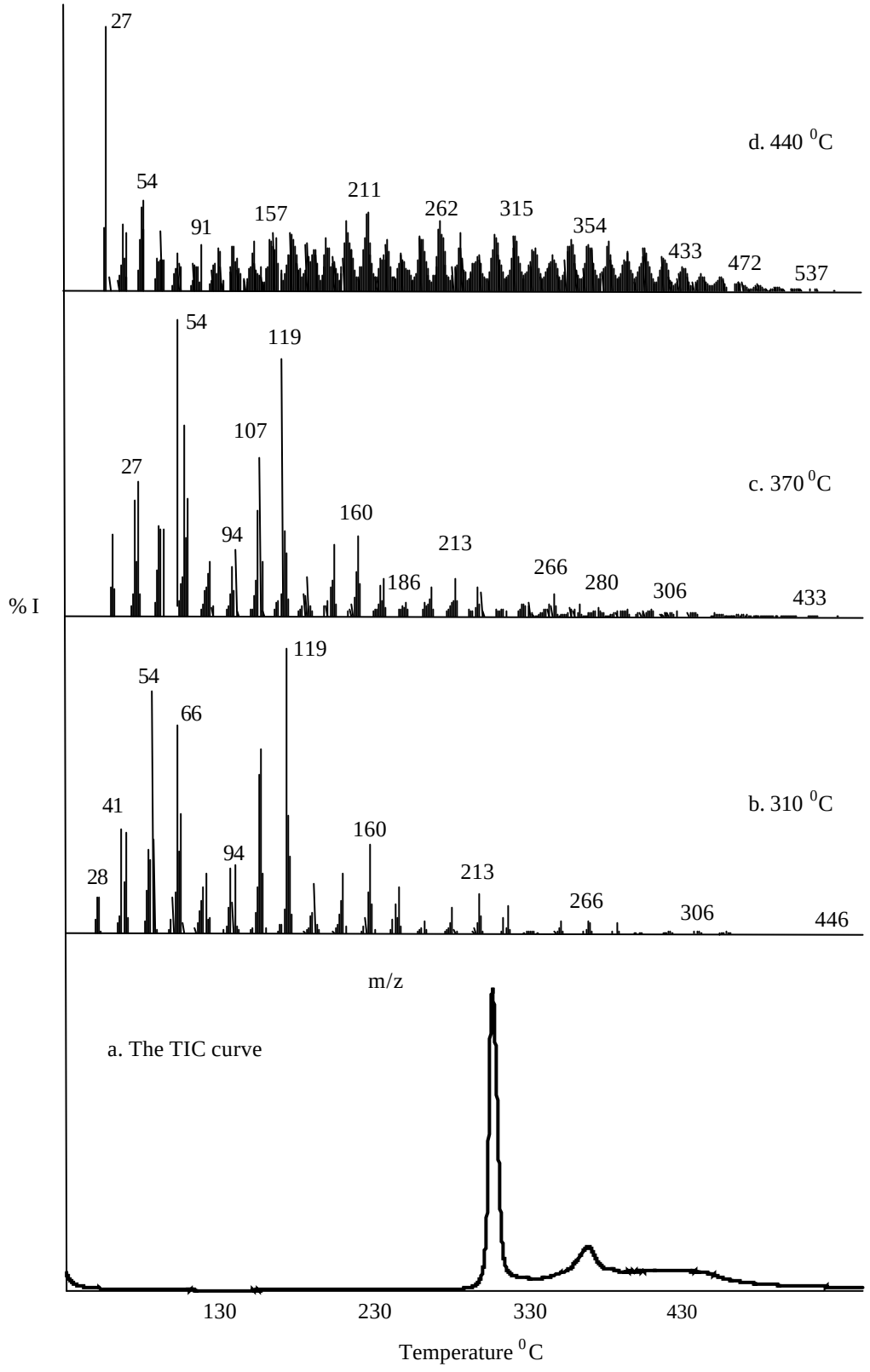

Figure III.1 a. The TIC curve and the mass spectra recorded at b. 310 ^{0}C, c. 370 ^{0}C, and d. 440 ^{0}C for PAN analyzed at high energy (70 eV)

In general, pyrolysis mass spectra are quite complicated due to the further dissociation of thermal degradation products during ionization. In order to determine the effects of dissociative ionization, the experiments were repeated decreasing the ionization energy from 70 eV to 19 eV. The 19 eV - TIC curve and the mass spectra recorded at the peak maxima of the TIC curve are given in Figure III.2. It is clear that 70 eV and 19 eV mass spectral data showed similar trends, that means, nearly the same product peaks were detected both in 70 eV and 19 eV pyrolysis mass spectra. The only difference noted was the increase in the relative intensities of the peaks due to fragments with low m/z ratios. Thus, it can be concluded that the secondary fragmentations during the ionization in the mass spectrometer were not so important. Relative intensities of some of the characteristics and/or intense peaks in the 70 and 19 eV pyrolysis mass spectra recorded at 310 ^{0}C, 370 ^{0}C and 440 ^{0}C and their assignments are given in Table III.1.

Actually, what is important for thermal and structural analysis is not the presence of a product peak but the variation of its intensity as a function of temperature. Thus, in order to get a better understanding of thermal degradation processes, single ion pyrograms, the variation of intensity of a product peak as a function of temperature, have been studied. In Figure III.3 and 4 evolution profiles of monomer, oligomers and some selected products are given. It can be observed from Figure III.3 that single ion pyrograms of monomer (m/z=54), dimer (m/z=107), trimer (m/z=160), tetramer (m/z=213) and pentamer (m/z=266) gave two maxima around 310 ^{0}C and 370 ^{0}C. In general, the products showing identical trends in their single ion pyrograms are generated by the same mechanism. Thus, it can be concluded that the monomer and the low molecular weight oligomers were formed through the same mechanism. Furthermore, it is noted that as the number of monomer units in the oligomer increased, its relative intensity decreased.

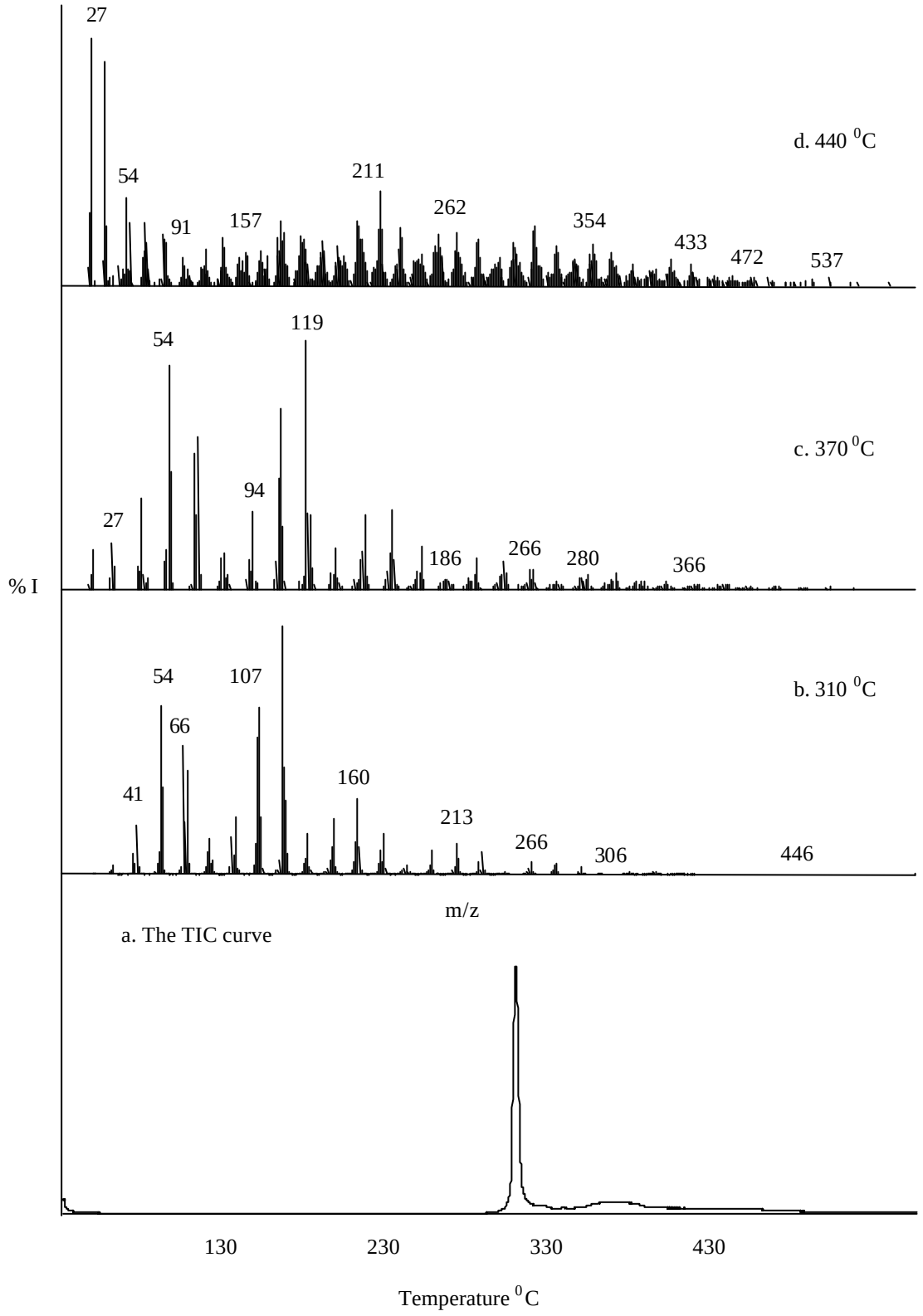

Figure III.2 a. The TIC curve and the mass spectra recorded at b. 310 ^{0}C, c. 370 ^{0}C, and d. 440 ^{0}C for PAN analyzed at low energy (19 eV)

Table III. 1. The characteristics and/or intense peaks present in the 70 and 19 eV pyrolysis mass spectra at the maxima of the TIC curves of PAN

m/z	Relative Yield						Assignment
	310 ^{0}C		370 ^{0}C		445 ^{0}C		
	19 eV	70 eV	19eV	70 eV	19 eV	70 eV	
27	19	129	226	301	806	880	HCN
41	182	361	382	506	253	328	CH_3CN, C_3H_5, NC_2H_3
54	652	845	865	1000	197	225	$(C_2H_3CN)H$
80	132	208	152	190	101	85	(C_2H_3CN)-C_2H_3
107	603	631	697	565	141	132	$(C_2H_3CN)_2H$
119	1000	1000	1000	895	141	105	$(C_2H_3CN)_2CH$
160	288	300	305	281	150	133	$(C_2H_3CN)_3H$
186	34	42	65	52	106	96	$(C_2H_3CN)_3$-C_2H_3
211	14	18	49	53	335	289	(C_2HCN)-$(C_2H_3CN)_3H$
213	115	135	104	134	129	132	$(C_2H_3CN)_4H$
239	8	11	22	28	110	96	$(C_2H_3CN)_4$-C_2H_3
262		1	31	28	324	263	$(C_2HCN)_2$-$(C_2H_3CN)_3H$
266	37	45	57	75	56	84	$(C_2H_3CN)_5H$
306	8	6	18	26	48	52	$(C_2HCN)_6$
366			3	7	109	162	$(C_2HCN)_3$-$(C_2H_3CN)_4H$
419					69	96	$(C_2HCN)_3$-$(C_2H_3CN)_5H$
526						17	$(C_2HCN)_3$-$(C_2H_3CN)_7H_2$

In Figure III.4, the single ion pyrograms of some intense and/or characteristic peaks recorded in the mass spectra of PAN are shown. Taking into consideration the similarities in the evolution profiles, it may be proposed that the fragments with m/z=186 and m/z=239 and the fragments with m/z=262 and m/z=419 at elevated temperatures were generated through the same mechanism. It can be clearly seen from the single ion pyrograms that the pyrolysis products having unsaturated bonds were generated at higher temperatures.

With the use of pyrolysis data the following thermal degradation mechanisms can be proposed. In Scheme III.1, the thermal degradation mechanism and the thermal degradation products occurred at 310 ^{0}C are given. According to this scheme, PAN degrades around 310 ^{0}C mainly through two different mechanisms; the cleavages at the α-carbon and loss of side groups. Possible thermal degradation mechanism taking place at elevated temperatures are given in Scheme III.2 and III.3.

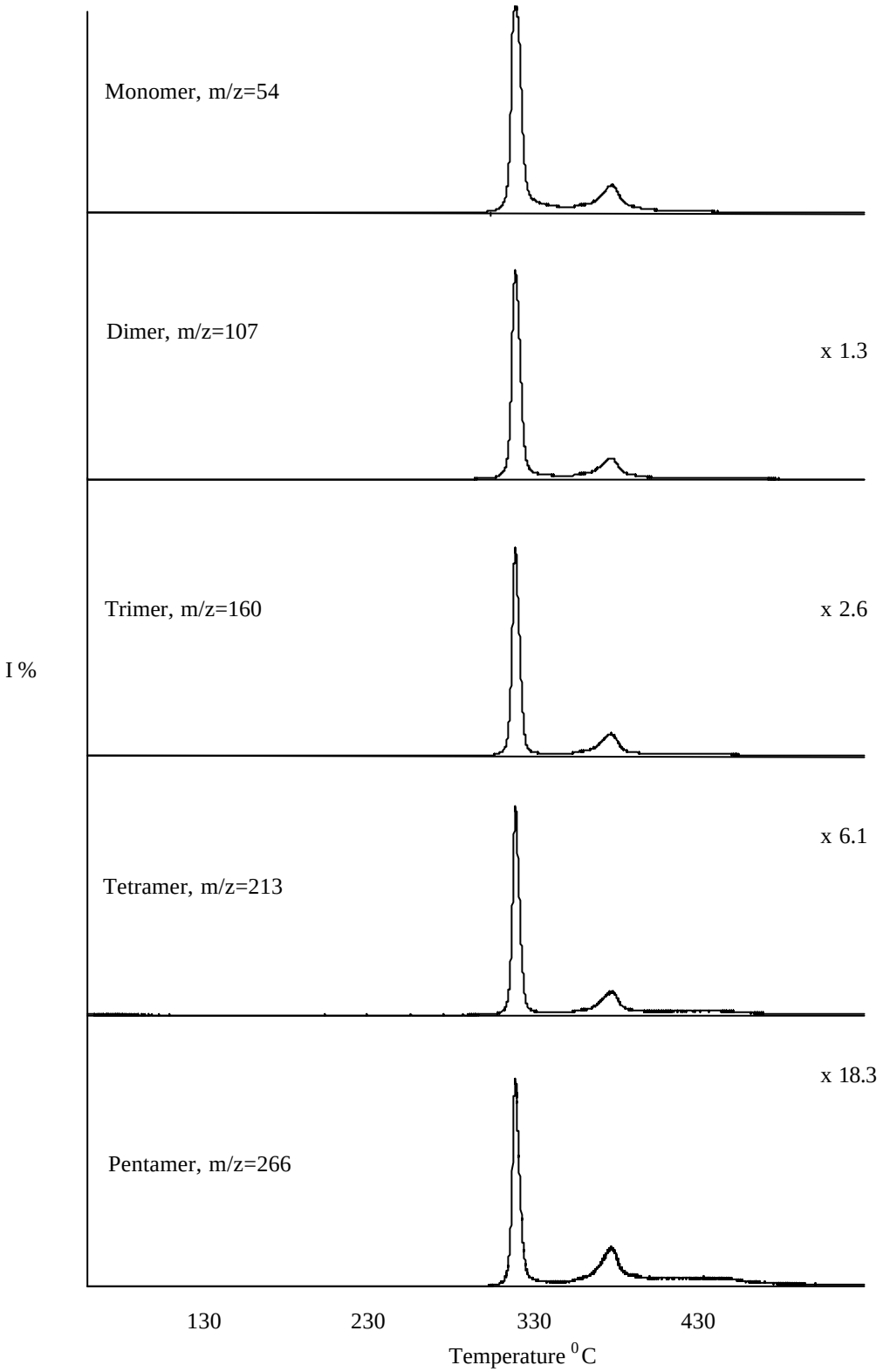

Figure III.3 Single ion pyrograms of monomer at m/z 54 Da and oligomers at m/z 107, 160, 213 and 266 Da during the pyrolysis of PAN

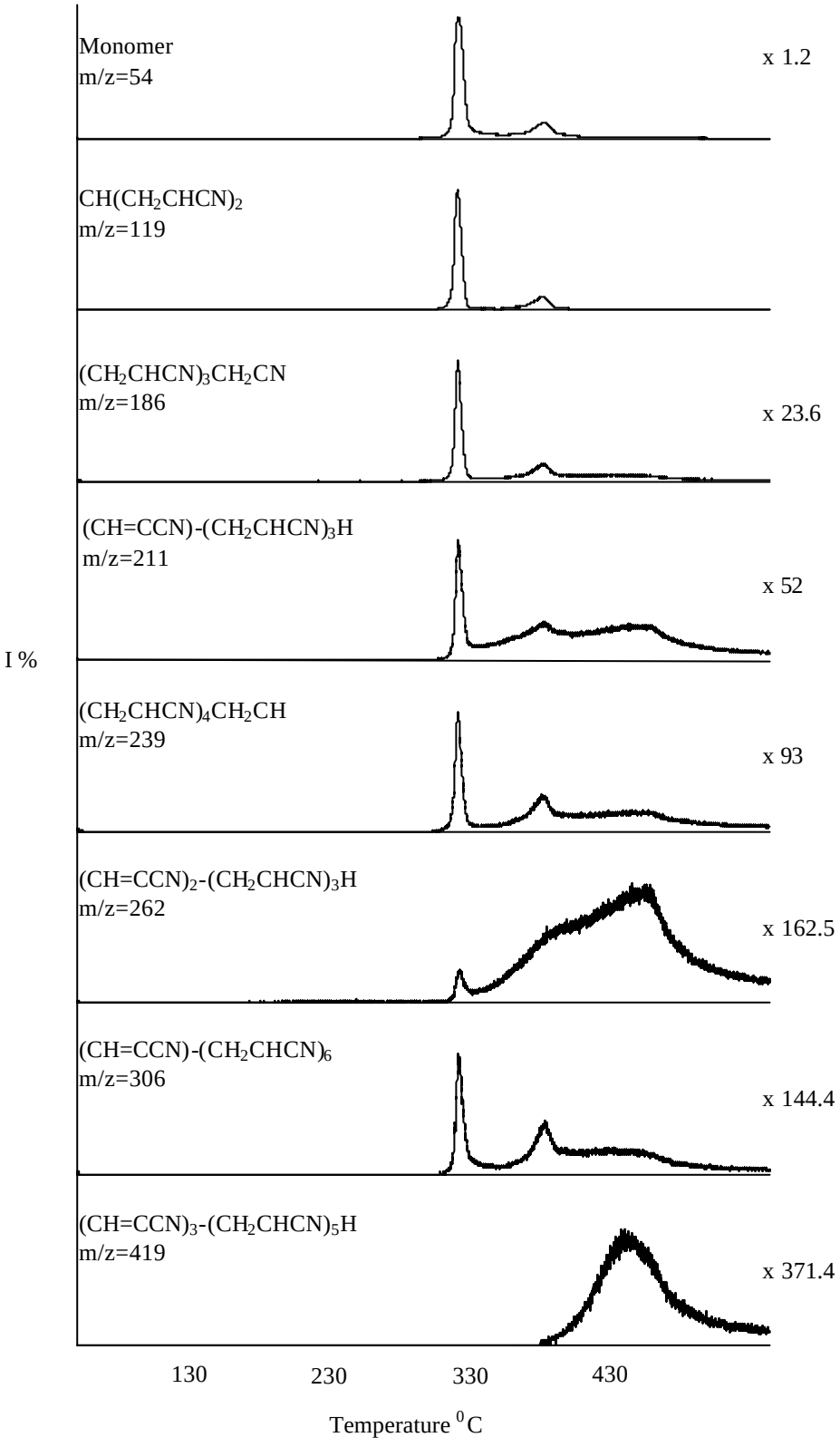

Figure III.4 Single ion pyrograms of the ions at m/z 54, 119, 186, 211, 239, 262, 306 and 419 Da during the pyrolysis of PAN

Scheme III.1 The thermal degradation mechanism of PAN at 310 ^{0}C

a) The cleavage at α-carbon

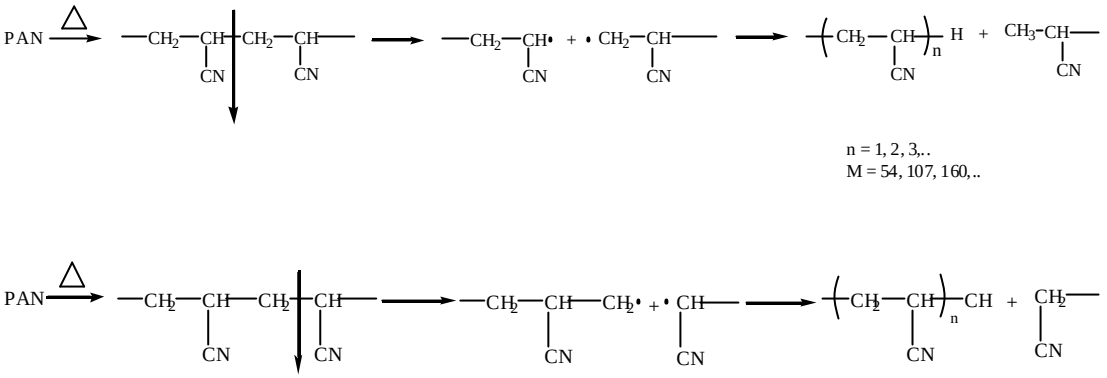

b) The cleavage of side groups

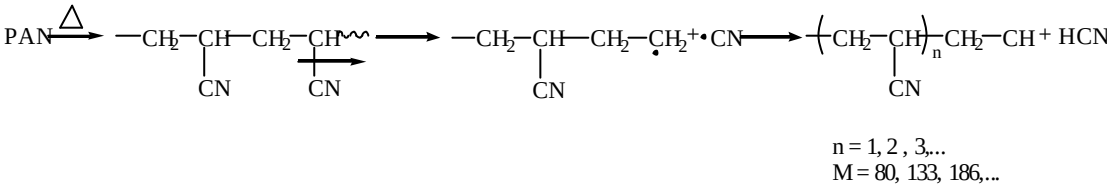

Scheme III.2 The generation of unsaturation and crosslinking around 370 ^{0}C

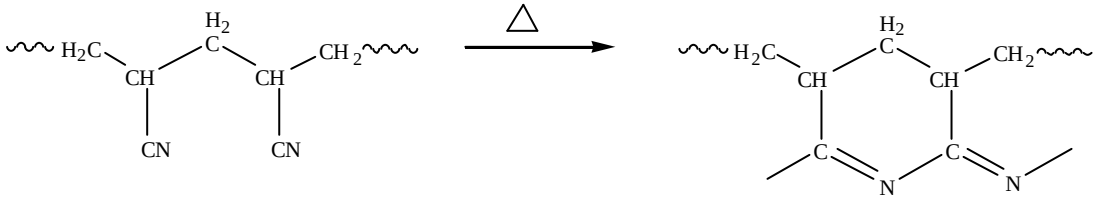

Scheme III.3 The thermal degradation mechanism of PAN at elevated temperatures

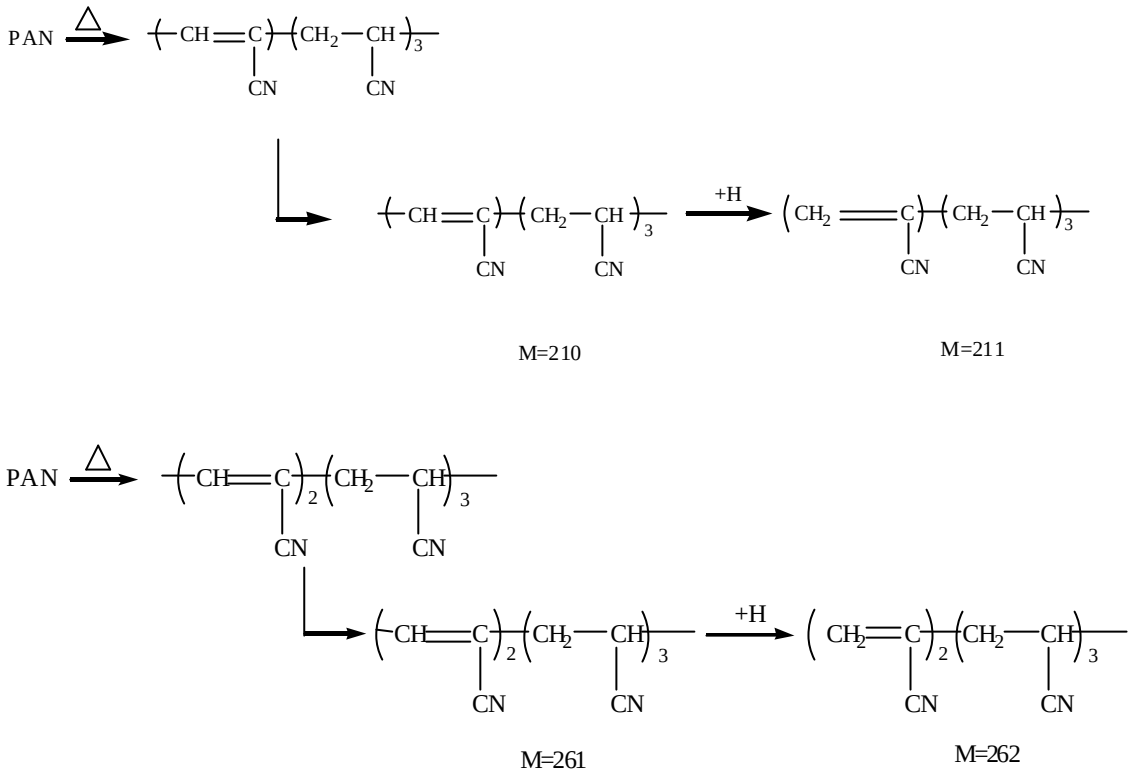

III.1.2. Polyacrylonitrile Films Treated Under Certain Experimental Conditions

In order to determine the applicability of PAN as a matrix for PTh, the effects of electrochemical synthesis conditions on the characteristics of PAN were investigated. For this purpose, PAN films were left in acetonitrile, and acetonitrile/TBABF solvent-electrolyte system for different time periods with or without applying 1.9 V potential to the working electrode coated with PAN.

In Figure III.5, the total ion current (TIC) curve of PAN film and PAN films treated under certain experimental conditions are shown. TIC curve of commercial PAN is also given for comparison.

Figure III.5.a and b show TIC curve of commercial PAN powder and PAN film obtained by dissolving PAN in DMSO respectively. TIC curve of PAN film left in

acetonitrile for 10 minutes is given in Figure III.5.c. Figure III.5.d.e.f., and g show the TIC curves of PAN films left in solvent-electrolyte system for 1, 5, 15 and 30 minutes, respectively while applying 1.9 V potential.

Analysis of pyrolysis data indicated that in general, upon film formation cyclization reactions are enhanced. Leaving the PAN film in acetonitrile did not yield any detectable change. However, significant differences exist between TIC curve of PAN powder and those of PAN films treated under different experimental conditions. When PAN films were left in solvent-electrolyte system while applying 1.9 V, structural changes have increased as a function of time. Analysis of the mass spectra and the single ion pyrograms indicated that the onset of pyrolysis shifted to higher temperatures. At low temperatures, below 310 ^{0}C, only a limited amount of products was formed. It can be concluded that as the time periods the polymer film left in solvent-electrolyte system increased, the polymer film became more homogeneous, with significant increase in unsaturation.

Figure III.6.a shows the single ion pyrograms of the ions at $(C_2H_3CN)_2CH$ (m/z=119 Da), $(C_2HCN)_3(C_2H_3CN)_4H$ (m/z=366Da), and $(C_2HCN)_3(C_2H_3CN)_5H$ (m/z=419Da) recorded during the pyrolysis of PAN powder and in Figure III.6.b, c and d, the single ion pyrograms of the same ions recorded during the pyrolysis of PAN films left in solvent-electrolyte system for 1, 5 and 30 minutes while applying 1.9 V potential, respectively are given. It can be seen from Figure III.6.b.c and d that as the time period the PAN films left in solvent-electrolyte system at 1.9 V potential increased, the generation of the high molecular weight fragments involving unsaturated segments enhanced at elevated temperatures.

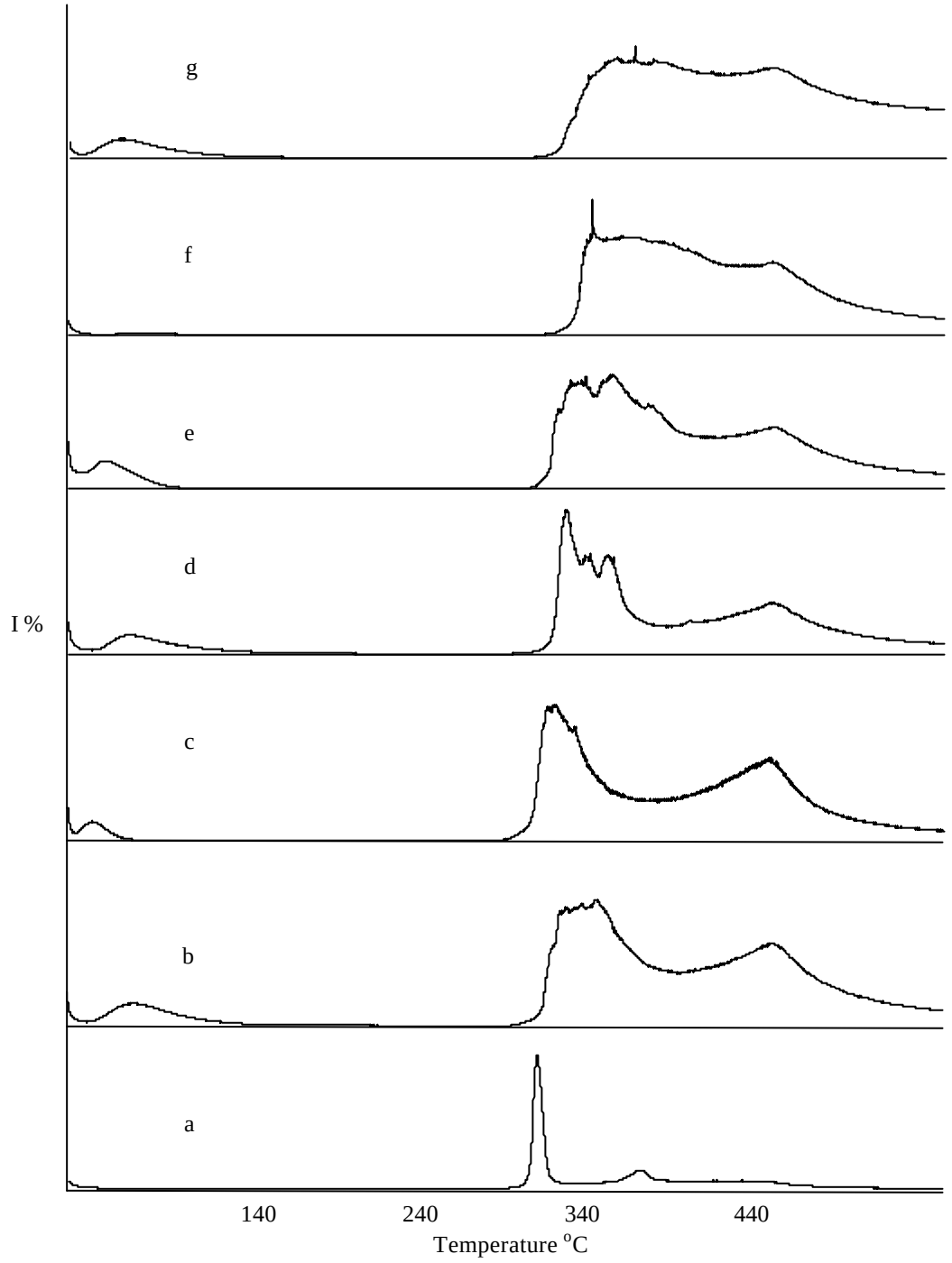

Figure III.5 Total Ion Current (TIC) curves of a. PAN powder, b. PAN film obtained by dissolving PAN powder in DMSO, c. PAN film left in acetonitrile for 10 min, and PAN films treated in solvent-electrolyte system at 1.9 V for d. 1 min e. 5 min f. 15 min and g. 30min

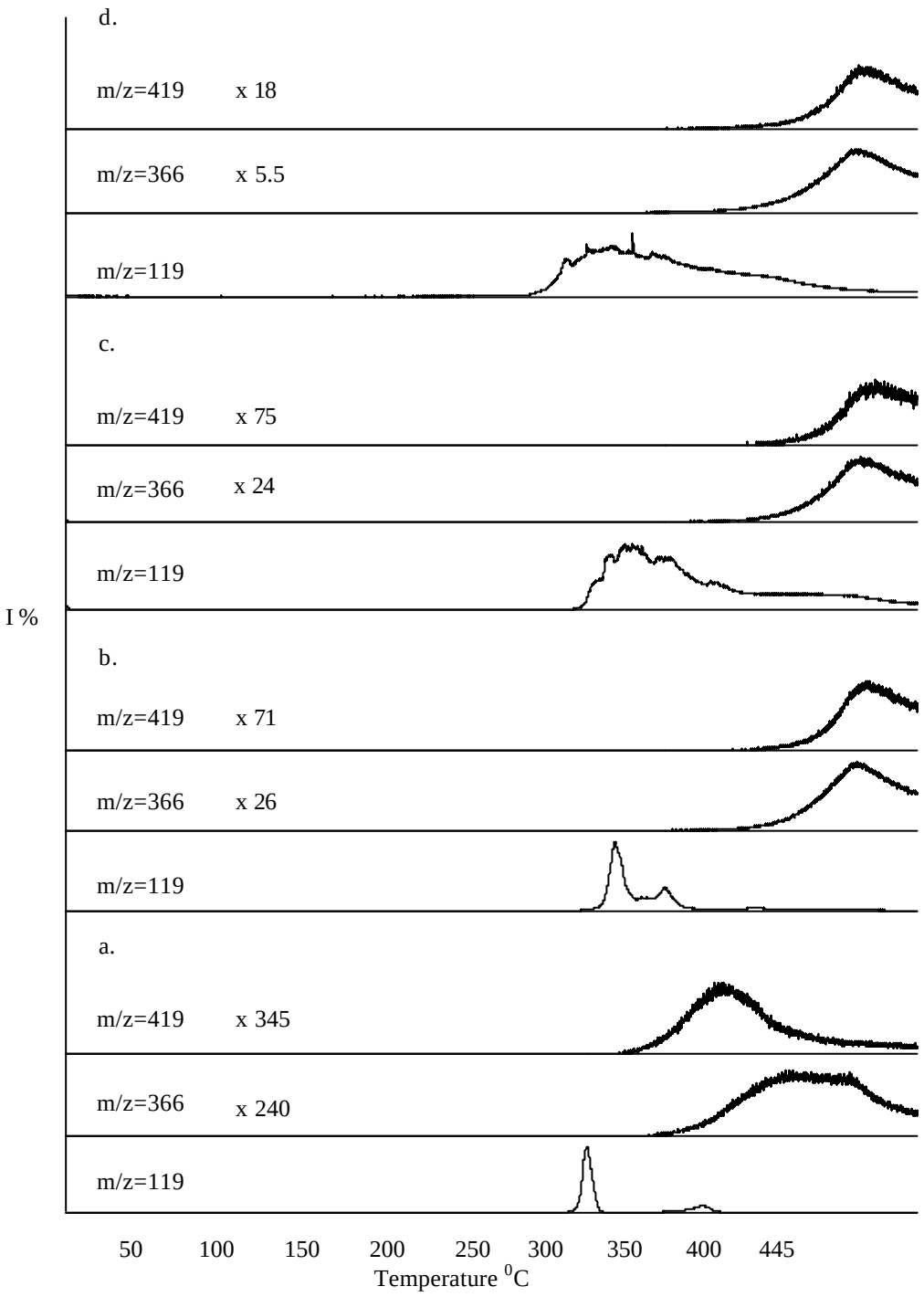

Figure III.6 Single ion pyrograms of the ions with m/z 119, 366 and 419 Da obtained during the pyrolysis of a. PAN powder and PAN films left in solvent-electrolyte system for b. 1 minute, c. 5 minutes d. 30 minutes, while applying 1.9 V potential

III.2. Polythiophene

The TIC of polythiophene (PTh) is given Figure III.7. Three peaks with maxima at 75, 250 and 445 ^{0}C can be seen in the TIC curve. The pyrolysis mass spectra recorded at these temperatures are also included in Figure III.7.

The pyrolysis mass spectra indicated that at initial stages of pyrolysis, at temperatures lower than 100 ^{0}C, the evolution of solvent, acetonitrile, water, dopant and its counter ion Bu_4N^+ adsorbed on the polymer film have occurred. Evolution of dopant based products was observed around 250 ^{0}C. Among these the most abundant fragment is BF_2^+ (m/z=49 Da) and its maximum yield was observed at 250 ^{0}C. Peaks that can be associated with thermal degradation of PTh were detected in the final stage of pyrolysis. Oligomer peaks up to six monomer units were present in the spectra. Moreover, in the final stage of pyrolysis, some peaks that can be associated with the cleavage of the thiophene (Th) ring such as peaks due to C_2H_2 (m/z=26 Da), S (m/z=32 Da), H_2S (m/z=34 Da), C_3H_3 (m/z=39 Da), HCS (m/z=45 Da), C_3H_3S (m/z=71 Da), $(C_2H_2S_2)_2$ (m/z=116 Da), $C_4H_3SCH_2$ (m/z=97 Da), C_4H_3S-C_4H_2S-CH_2 (m/z=179 Da) and C_4H_3S-$(C_4H_2S)_2$-C_2H_2 (m/z=273) were also recorded. The relative intensities of some of the characteristics and/or intense peaks present in the pyrolysis mass spectra recorded at 250 and 445^{0}C and their assignments are given in Table III.2.

In Figure III.8 and 9, evolution profiles of some selected products are given. It can be observed from Figure III.8. that the single ion pyrograms of low molecular weight products, dimer (m/z=166 Da), trimer (m/z=248 Da), tetramer (m/z=330 Da), pentamer (m/z=412 Da) and hexamer (m/z=494 Da) gave maximum around 445^{0}C. However, as the monomer unit in the oligomer increased, the evolution profiles shifted to higher temperatures and the tail at the low temperature side of the profile diminished significantly.

The single ion pyrograms of some dopant based products, such as HF (m/z=20 Da), BF_2 (m/z=49 Da), BF_3 (m/z=68 Da), counter ion Bu_4N^+ (m/z=242) and $(C_4H_9)_2H$=CH_2 (m/z=142 Da) are shown in Figure III.9. BF_3 and BF_2 fragments

showed identical trends and the maximum in the evolution profiles is at 250 ^{0}C. Yet, HF generation was more efficient at low temperatures. It is known that reactions of BF_3 with H_2O yields HF. Thus it may be proposed that HF mainly produced due to reactions with adsorbed water, as shown in Scheme III.4.

Scheme III.4. The generation of HF

$6H_2O \rightarrow 4H_3O^+ + 4e^- + O_2$

$PTh^+\text{-}BF_4^- + H_3O^+ + e^- \rightarrow PTh + HBF_4 + H_2O$

$HBF_4 \rightarrow HF + BF_3$

It is clear that the peak around 250 ^{0}C in the TIC curve was due to the evolution of dopant and the peak above 400 ^{0}C was due to the decomposition of PTh chains. Another point that was noted is the presence of peaks due to counter ion NBu_4^+. Unfortunately, the extent of adsorption was quite high and peaks due to alkyl fragments were also detected at elevated temperatures, although, the samples were washed several times with the solvent. It may be thought that these substances were trapped in the bulk of the polymer during the electrochemical deposition. Previous TGA and FTIR studies have also shown that the degradation of PTh occurs in two steps. The first one is the weight loss in the temperature range 150-225 ^{0}C being due to the loss of dopant and the second one at high temperatures in the range of 400-600 ^{0}C being due to the degradation of the polymer itself [27-28].

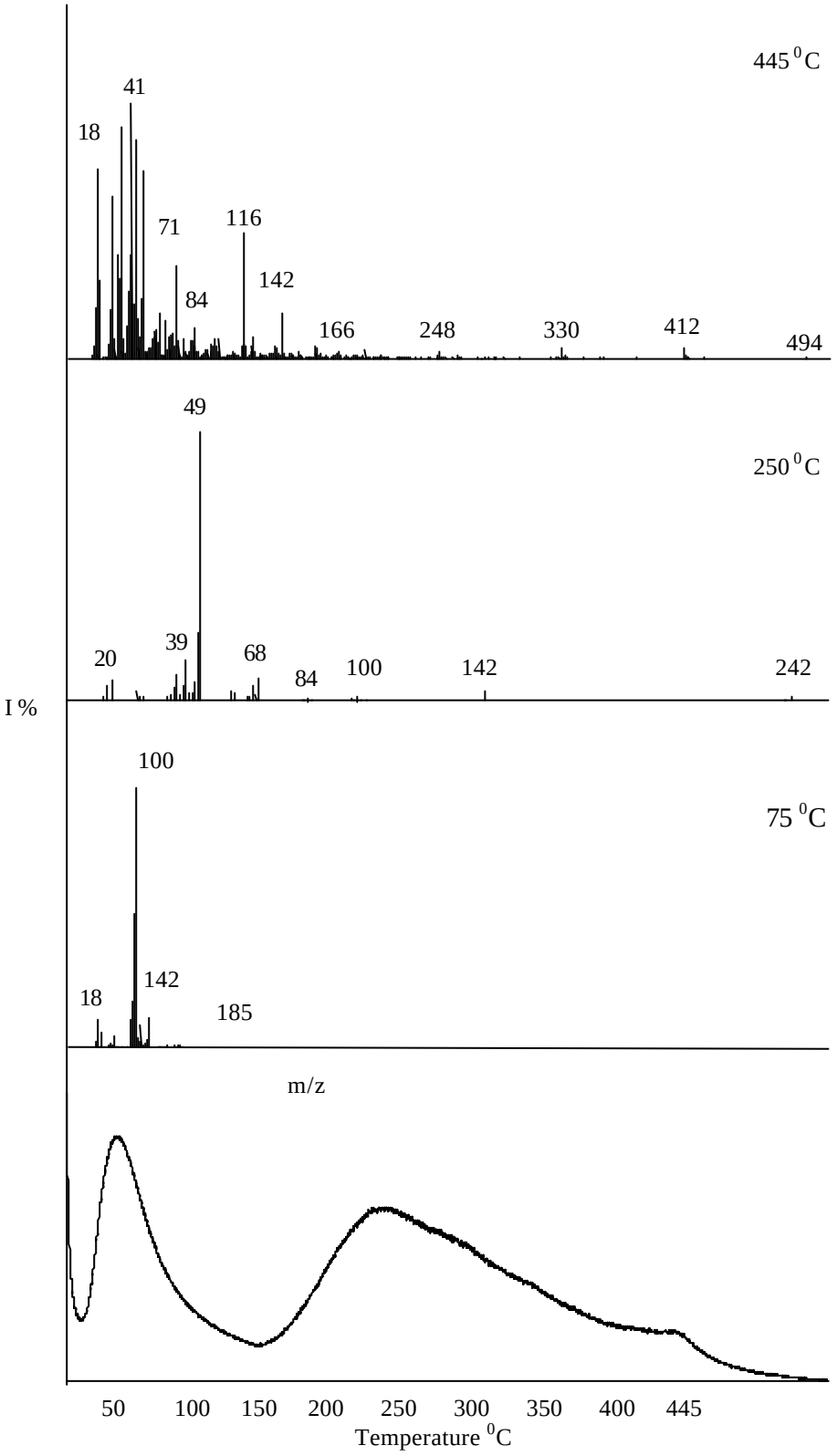

Figure III.7 TIC curve and mass spectra recorded at temperatures corresponding to the peak maxima for BF_4^- doped PTh analyzed at high energy (70 eV)

Table III.2 The characteristics and/or intense peaks present in the pyrolysis mass spectra corresponding to the maximum in the TIC curve recorded during the pyrolsis of BF_4^- doped PTh

m/z	Relative Yield		Assignment
	250 ^{0}C	445 ^{0}C	
20	72	311	HF
26	3	60	C_2H_2
28	34	640	CO, N_2, C_2H_4
30	9	35	BF, CH_2=O
34	2	910	H_2S
39	19	264	C_3H_3
41	95	1000	CH_3CN, C_3H_5, NC_2H_3
44	145	857	CO_2, CS
45	25	160	CHS
49	1000	738	BF_2
60	24	179	OCS
64	12	153	SO_2
68	78	97	BF_3
71	3	362	C_3H_3S
84	6	121	Monomer
85	1	27	$CH_2C_4H_9N$
97	1	76	$CH_2C_4H_3S$
101	1	7	FC_4H_2S
102	1	9	FC_4H_3S
116	1	493	$(C_2H_2S_2)_2$
122	1	47	$C_3H_3C_4H_3S$
142	36	177	$(C_4H_9)_2N$=CH_2, $(C_3H_3S)_2$
166		43	Dimer
179		26	$C_4H_3SC_4H_2SCH_2$
242	10	6	$(C_4H_9)_4N$
248		30	Trimer
330		42	Tetramer
412		42	Pentamer
494		7	Hexamer

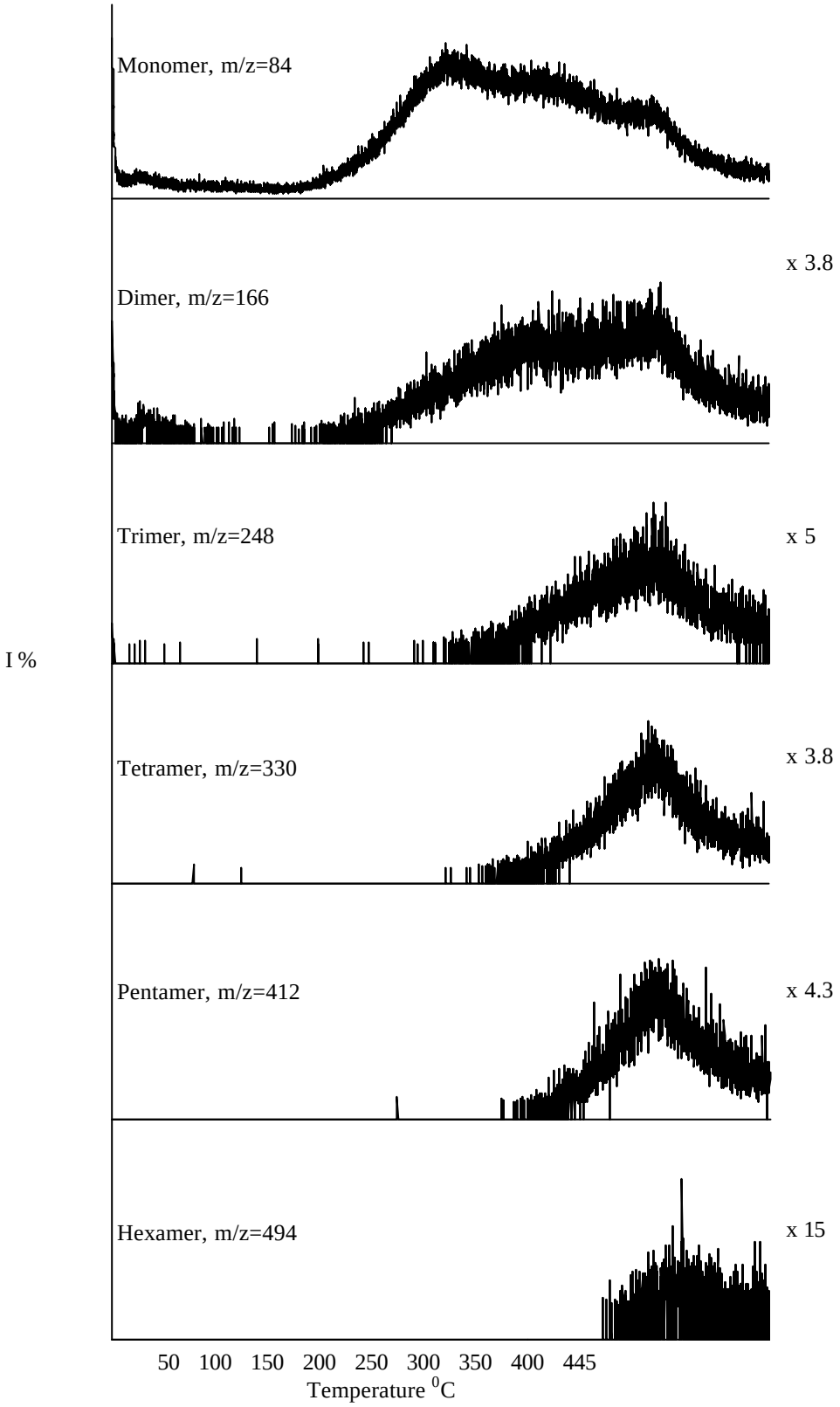

Figure III.8 Single ion pyrograms of monomer and the oligomers at m/z 84, 166, 248, 330, 412 and 494 Da respectively recorded during the pyrolysis of BF_4^- doped PTh.

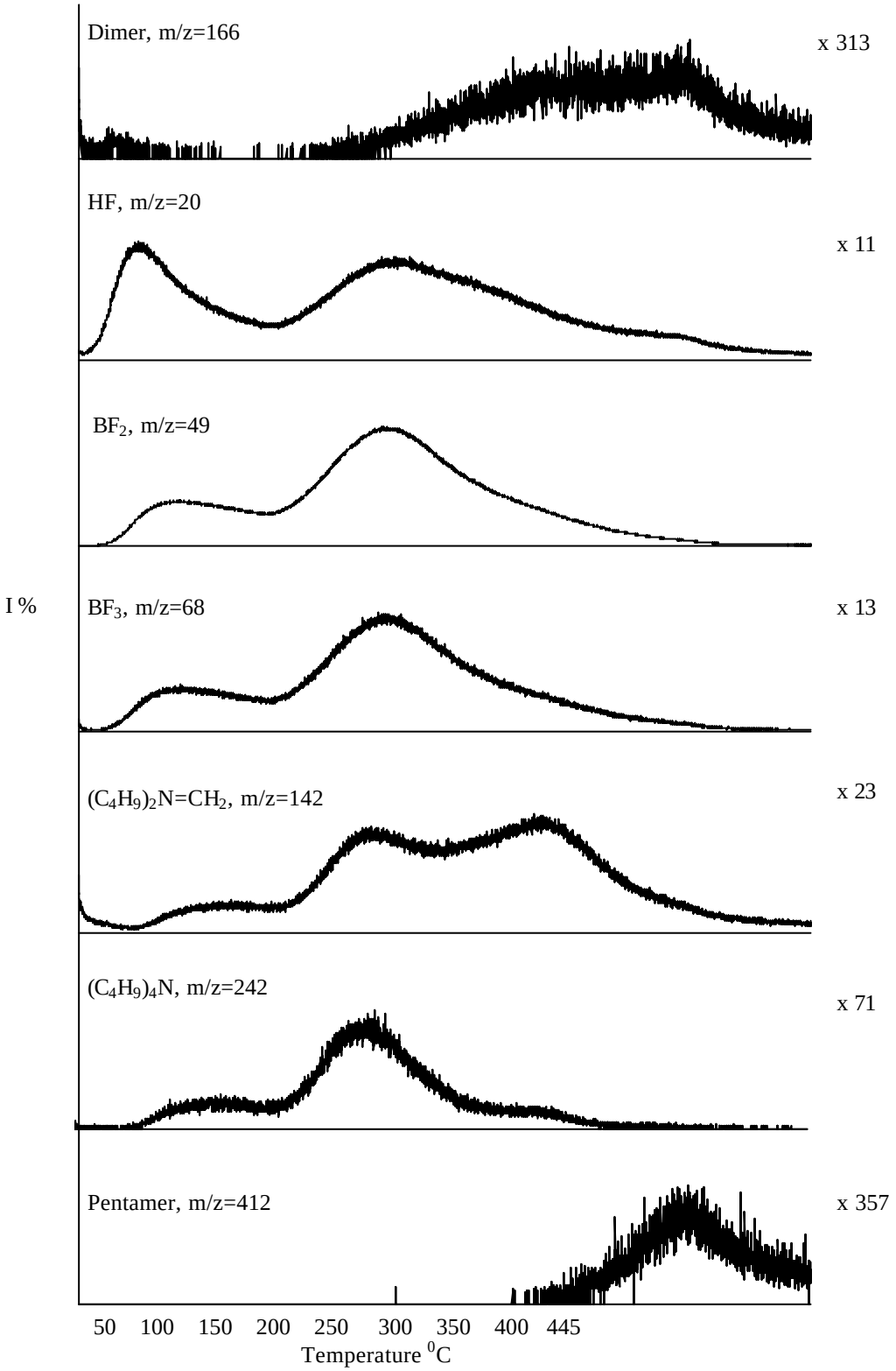

Figure III.9. Single ion pyrograms of the ions at m/z 166, 20, 49, 68, 142, 242 and 412 Da recorded during the pyrolysis of BF_4^- doped PTh

III.3.Polybutadiene

Pyrolysis mass spectrometry analysis of polybutadiene (PB) has also been performed. The TIC curve and the pyrolysis mass spectra of PB recorded at the maximum of the peaks in the TIC curve are given in Figure III.10. Two peaks with maximum at 270 and 400 ^{0}C and one shoulder at 445 ^{0}C can be seen in the TIC curve. The mass spectra recorded at these temperatures are also included in Figure III.10.

Analyses of the pyrolysis mass spectra recorded around 400 ^{0}C indicated that PB is degraded by radical homolytic chain scissions followed by dehydrogenation and cyclization reactions in accordance with the literature results. Besides the monomer and oligomer peaks up to thirteen monomer units $(C_4H_6)_{13}$ and fragments were also recorded. In general, the relative intensities of oligomer peaks decreased as the number of monomer units present increased. The base peak in the pyrolysis mass spectra was at m/z=79 Da due to C_6H_7. Thus, it may be proposed that cyclization reactions were effective in stabilization of the decomposition products. In Table III.3 the related mass spectral data is summarized.

Inspection of single ion pyrograms indicated that all the thermal degradation products show similar trends thus they were generated through the same degradation mechanisms. In Figure III.11, evolution profiles of some characteristic products at m/z=54 Da due to monomer (C_4H_6), m/z=67 Da due to C_5H_7, m/z=79 Da due to C_6H_7, m/z=324 Da due to $(C_4H_6)_6$ and m/z=540 Da due to $(C_4H_6)_{10}$ are shown.

Table III.3. The characteristics and/or intense peaks present in the pyrolysis mass spectra corresponding to the maximum in the ion profiles recorded during the pyrolysis of PB

m/z	Relative Yield			Assignment
	270 ^{0}C	400 ^{0}C	445 ^{0}C	
27	22	90	128	C_2H_3, HCN
41	238	277	518	C_3H_5
54	44	319	123	C_4H_6
57	1000	55	82	C_4H_9
79	149	1000	981	C_6H_7
91	332	707	1000	C_7H_7
97	132	44	82	C_7H_{13}
108	25	166	282	dimer
162	9	117	129	trimer
185	20	86	107	$(C_4H_6)_2C_6H_5$
216	9	45	60	tetramer
255	12	41	37	$(C_4H_6)_4C_3H_3$
270	9	31	31	pentamer
295		22	23	$(C_4H_6)_4C_6H_7$
324		22	17	hexamer
336		6	11	$(C_4H_6)_6CH_2$
364		11	11	$(C_4H_6)_6C_3H_4$
391		7	9	$(C_4H_6)_6C_5H_7$
401		3	9	$(C_4H_6)_6C_6H_5$
417	5	8	9	$(C_4H_6)_7C_3H_3$
540		8	2	$(C_4H_6)_{10}$
567		1	3	$(C_4H_6)_{10}C_2H_3$

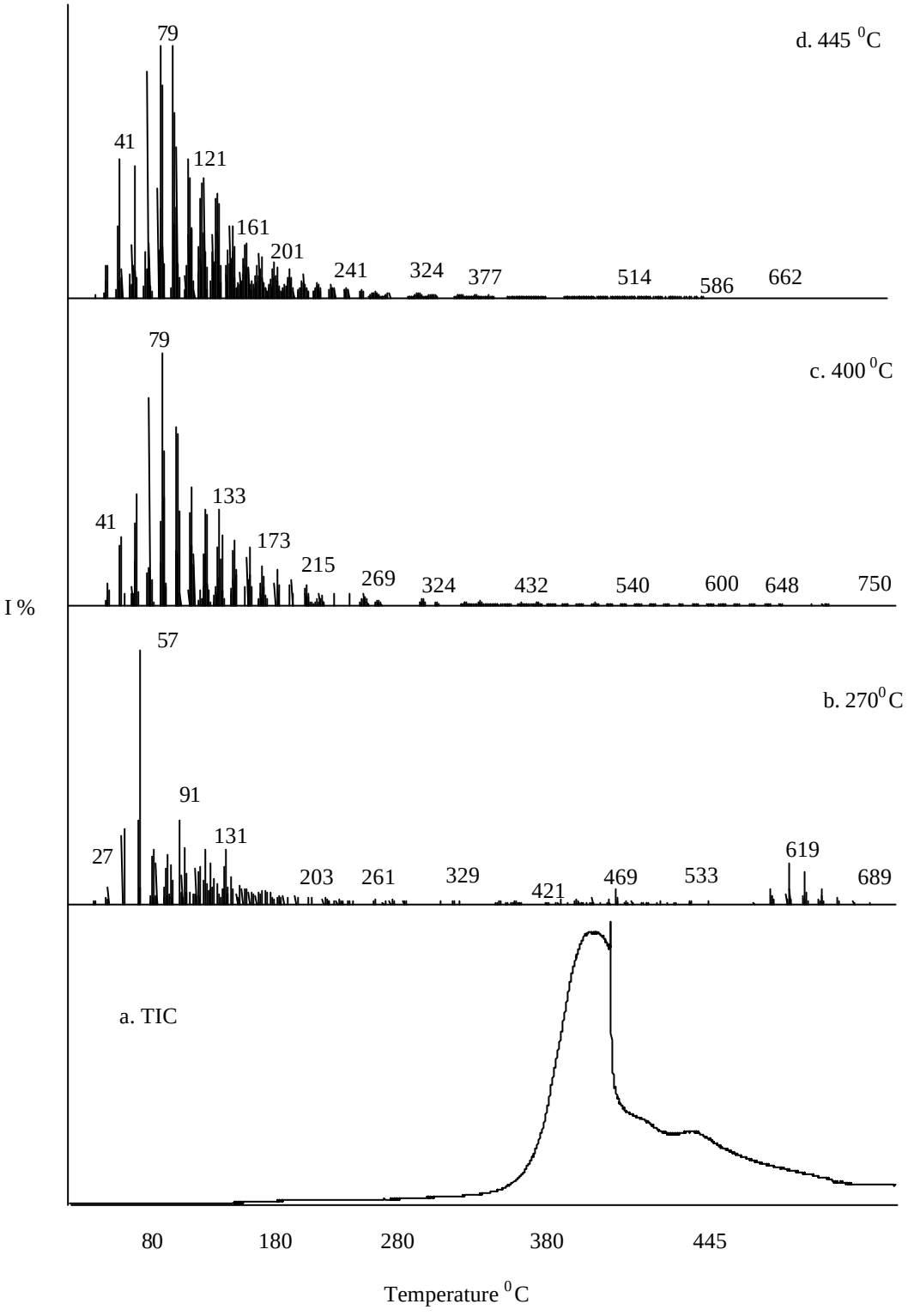

Figure III.10 a. The TIC curve and the mass spectra recorded at b. 270 ^{0}C, c. 400 ^{0}C, and d. 445 ^{0}C during the pyrolysis of PB

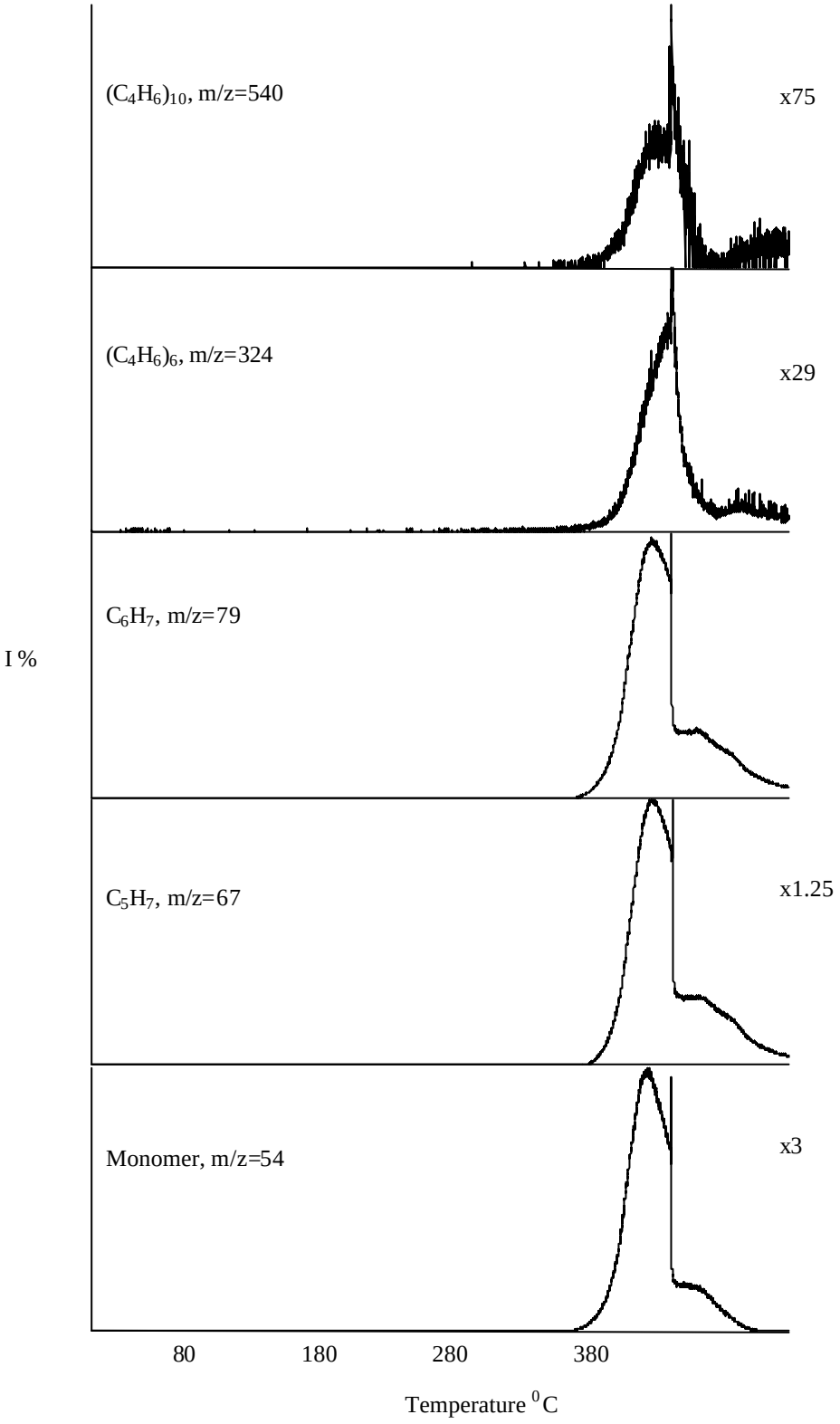

Figure III.11 Single ion pyrograms of the ions at m/z 540, 324, 79, 67, and 54 Da recorded during the pyrolysis of PB

III.4. Copolymer of Polythiophene and Polyacrylonitrile (PTh/PAN)

In this section, the results of direct insertion probe pyrolysis mass spectrometry analyses of electrochemically prepared PTh/PAN films and the mechanical mixture of PTh and PAN were discussed.

The total ion current (TIC) curve recorded during the pyrolysis of electrochemically prepared PTh/PAN film is shown in Figure III.12, together with the TIC curves for the mechanical mixture and the corresponding homopolymers PAN and PTh. It is clear that the TIC curve of PTh/PAN is significantly different than all of the others, whereas that of the mechanical mixture is quiet similar to that of PAN. However, the pyrolysis mass spectra of both PTh/PAN and the mechanical mixture were dominated with diagnostic peaks of both PTh and PAN. The pyrolysis mass spectra recorded at the maxima of the TIC curves of the mechanical mixture and PAN/PTh are shown in Figures III.13 and 14, respectively. Although the TIC curve of PAN showed no resemblance to that of PTh, peaks due to evolution of dopant and degradation of polythiophene were detected. Thus, presence of both components in both mechanic mixture and PAN/PTh was confirmed.

In general, evolution of the dopant, BF_4^-, based products were recorded around 240-250 ^{0}C for both PTh/PAN and the mechanical mixture. Above 300 ^{0}C diagnostic peaks of PAN appeared in the spectra, and in the final stages of pyrolysis, peaks not only due to the decomposition of polythiophene but also due to the fragments involving cyclic and unsaturated structures associated with thermal degradation of PAN were detected. Although similar peaks were present in both of the pyrolysis mass spectra of PTh/PAN and the mechanical mixture, the relative intensities of the product peaks showed drastic variations.

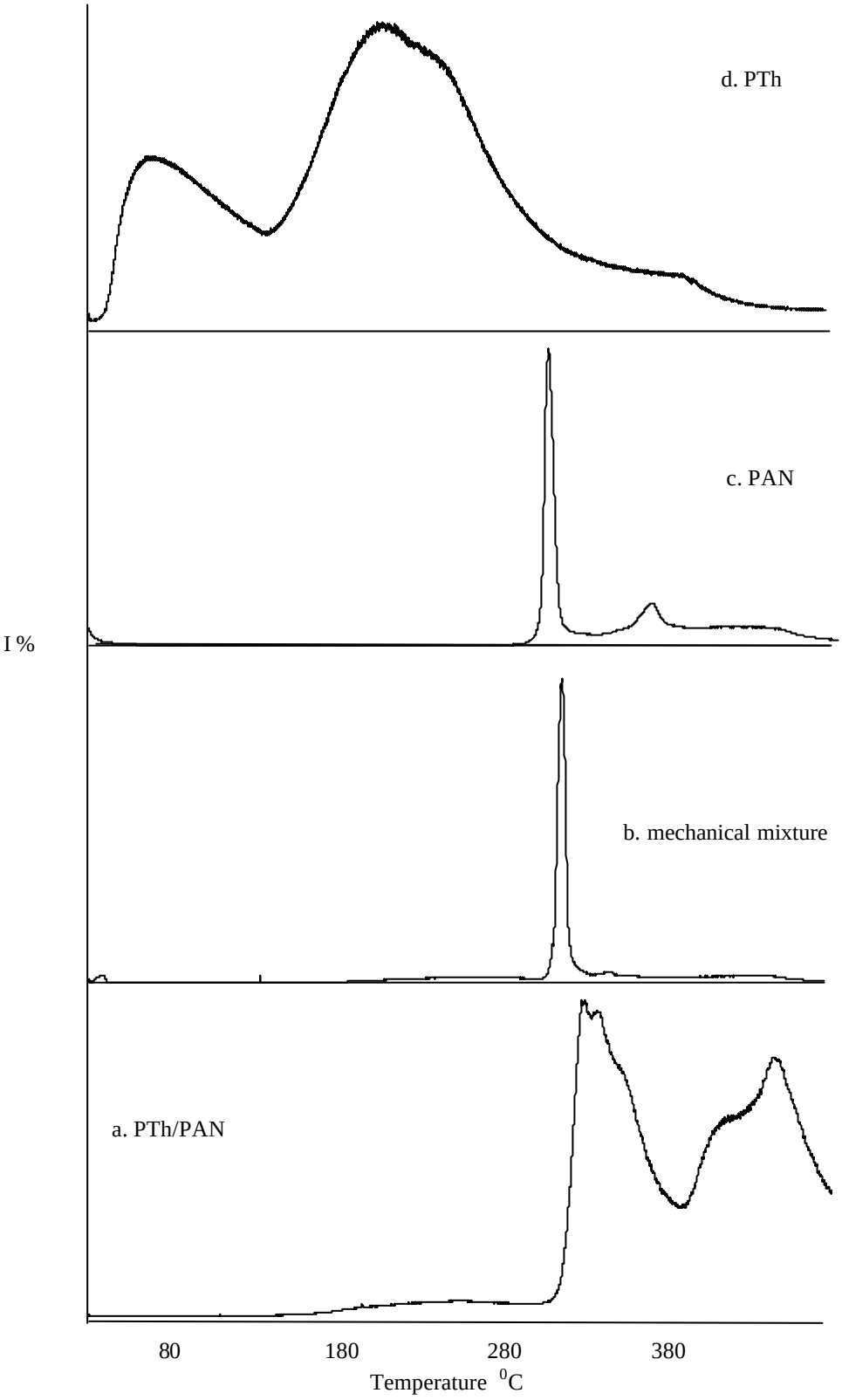

Figure III.12 TIC curve recorded during the pyrolysis of a. electrochemically prepared PTh/PAN film, b. mechanical mixture and corresponding homopolymers c. PAN and d. PTh

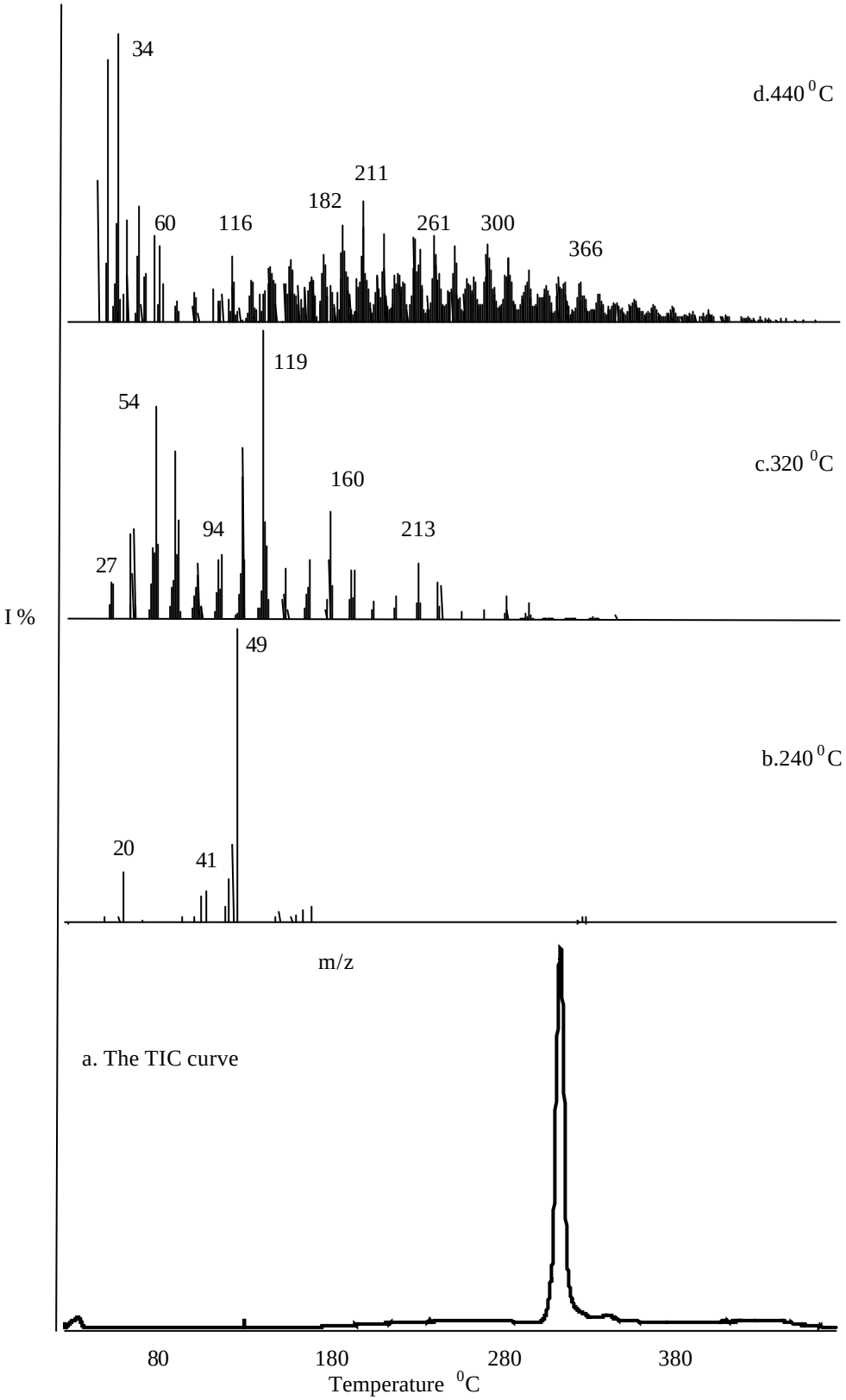

Figure III.13 a. TIC curve and the mass spectra recorded at b. 270 ^{0}C, c. 320 ^{0}C, and d. 440 ^{0}C during the pyrolysis of mechanical mixture PTh/PAN

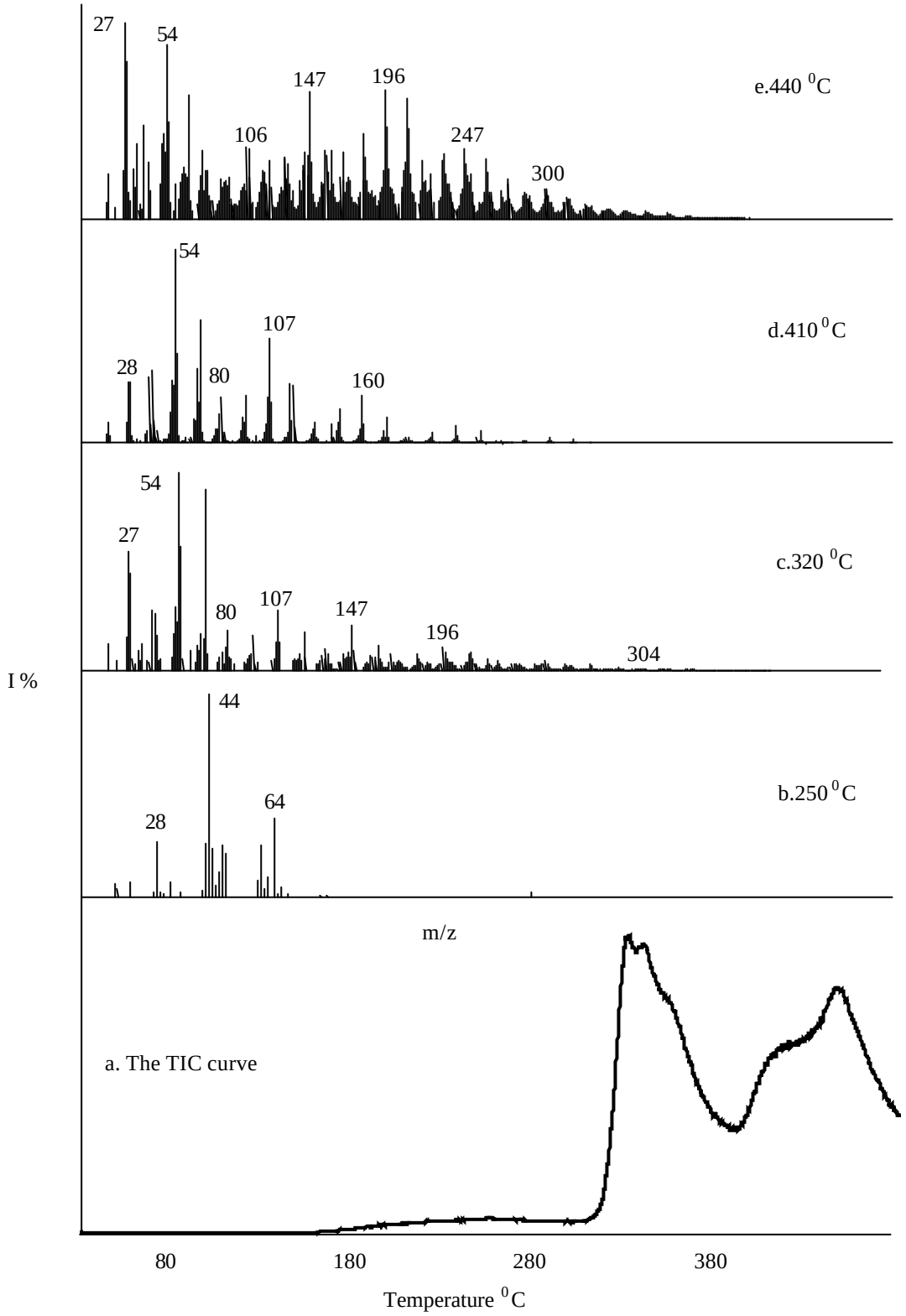

Figure III.14 a. TIC curve and the mass spectra recorded at b. 250 ^{0}C, c. 320 ^{0}C, d. 410 ^{0}C and e. 440 ^{0}C during the pyrolysis of PTh/PAN

The intense and/or characteristics peaks recorded in the pyrolysis mass spectra recorded at the maxima of the TIC curves of the mechanical mixture and PTh/PAN are summarized in Table III.4 and 5, respectively.

Actually, the analyses of pyrolysis data were quite complicated as degradation of both PAN and BF_4^- doped PTh yielded several products over a wide temperature range. What is more important for pyrolysis mass spectrometry analysis is not the presence of a product peak, but the variation of its intensity as a function of temperature that is its evolution profile. Thus, the evolution profiles of all characteristic thermal decomposition products generated during the pyrolysis of PTh/PAN and the mechanical mixture were studied and compared with those recorded from the corresponding homopolymers. Among the several products HCN (m/z=27 Da), $(C_2H_3CN)H$, (m/z=54 Da), $(C_2H_3CN)_2CH$ (m/z=119 Da), $(C_2H_3CN)_4H$ (m/z=211 Da) generated by the homolytic cleavages and $(C_2H_3CN)_2(C_2HCN)_2CH_2CN$ (m/z=248 Da) and $(C_2HCN)_3(C_2H_3CN)_5$ (m/z=418 Da) due to the degradation of dehydrogenated cyclic fragments were selected. On the other hand, for BF_4^-doped PTh component and HF and BF_2 (m/z=20 and 49 Da respectively) due to evolution of dopant, the thiophene trimer (m/z=248 Da) and H_2S (m/z=34 Da) associated with the cleavage of the thiophene ring were chosen as reference degradation products. The single ion pyrograms of these products recorded during the pyrolysis of mechanical mixture and electrochemically prepared BF_4^- doped PAN/PTh samples are given in Figures 15 and 16 respectively. The fragment with m/z=248 Da was generated from both PTh and PAN, thus for convenience, the evolution profile of this fragment is given twice. Furthermore, the evolution profiles of these products from PAN and PTh are also included in the figures for comparison.

Table III.4. The intense and/or characteristics peaks recorded in the pyrolysis mass spectra recorded at the maxima of the TIC curves of the mechanical mixture

m/z	Relative Yield			Assignment
	270 ^{0}C	330 ^{0}C	445 ^{0}C	
20	205	4	57	HF
27	31	138	114	HCN
34	5		101	H_2S
41	325	333	109	CH_3CN, C_3H_5, NC_2H_3
49	1000	27	31	BF_2
54	3	759	29	$(C_2H_3CN)H$
116	1	43	26	$(C_2H_2S_2)_2$
119	5	1000	13	$(C_2H_3CN)_2CH$
135	6	24	11	C_2H_3CN-C_4H_2S
160		388	16	$(C_2H_3CN)_3H$
188		11	12	$(C_2H_3CN)_2$-C_4H_2S
211	1	29	37	(C_2HCN)-$(C_2H_3CN)_3H$
213		207	13	$(C_2H_3CN)_4H$
217			5	C_2H_3CN-$(C_4H_2S)_2$
248		1	25	$(C_4H_2S)_3H_2$, $(C_2H_3CN)_4(C_2HCN)CH_2CN$
270			7	$(C_2H_3CN)_2$-$(C_4H_2S)_2$
306			22	$(C_2HCN)_6$
366			12	$(C_2HCN)_3$-$(C_2H_3CN)_4H$
418			5	$(C_2HCN)_3$-$(C_2H_3CN)_5$

Table III.5. The intense and/or characteristics peaks recorded in the pyrolysis mass spectra recorded at the maxima of the TIC curves of PTh/PAN

m/z	Relative Yield				Assignment
	260 ^{0}C	330 ^{0}C	410 ^{0}C	445 ^{0}C	
20	162	29	105	167	HF
27	39	316	615	1000	HCN
34	20	15	149	378	H_2S
41	242	663	935	996	CH_3CN, C_3H_5, NC_2H_3
49	184	35	30	38	BF_2
54	3	1000	1000	875	$(C_2H_3CN)H$
116	2	31	69	247	$(C_2H_2S_2)_2$
119	1	315	90	173	$(C_2H_3CN)_2CH$
135	1	19	37	95	C_2H_3CN-C_4H_2S
160		243	58	148	$(C_2H_3CN)_3H$
188		9	36	107	$(C_2H_3CN)_2$-C_4H_2S
211		14	99	440	(C_2HCN)-$(C_2H_3CN)_3H$
213		95	36	134	$(C_2H_3CN)_4H$
217		1	14	64	C_2H_3CN-$(C_4H_2S)_2$
248		2	31	275	$(C_4H_2S)_3H_2$, $(C_2H_3CN)_4(C_2HCN)CH_2CN$
270			6	50	$(C_2H_3CN)_2$-$(C_4H_2S)_2$
306		1	14	143	$(C_2HCN)_6$
366			1	32	$(C_2HCN)_3$-$(C_2H_3CN)_4H$
418				6	$(C_2HCN)_3(C_2H_3CN)_5$

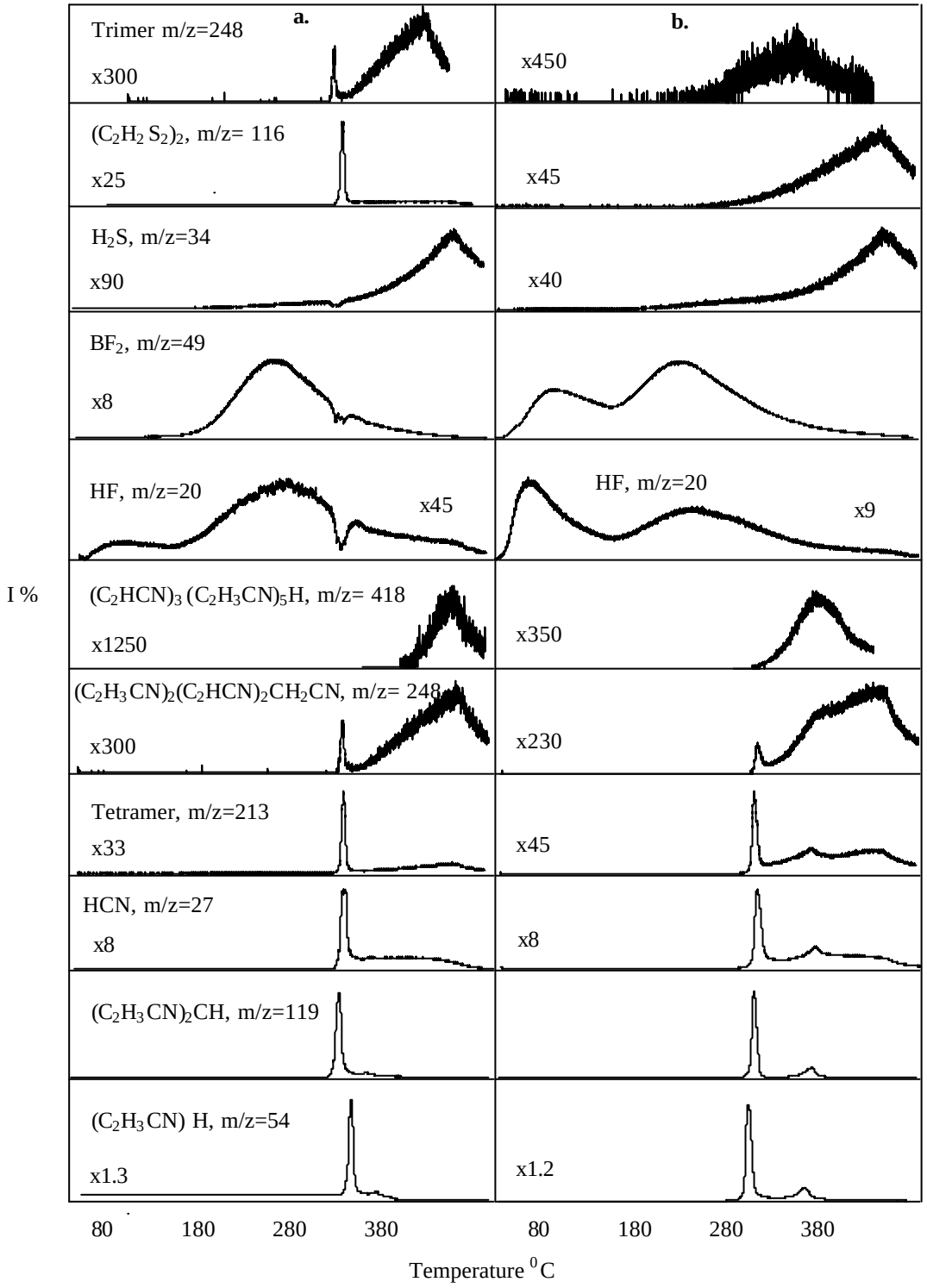

Figure III.15 The single ion pyrograms of some characteristic thermal decomposition products of a. polythiophene and polyacrylonitrile chains generated during the pyrolysis of the mechanical mixture, b. corresponding homopolymers

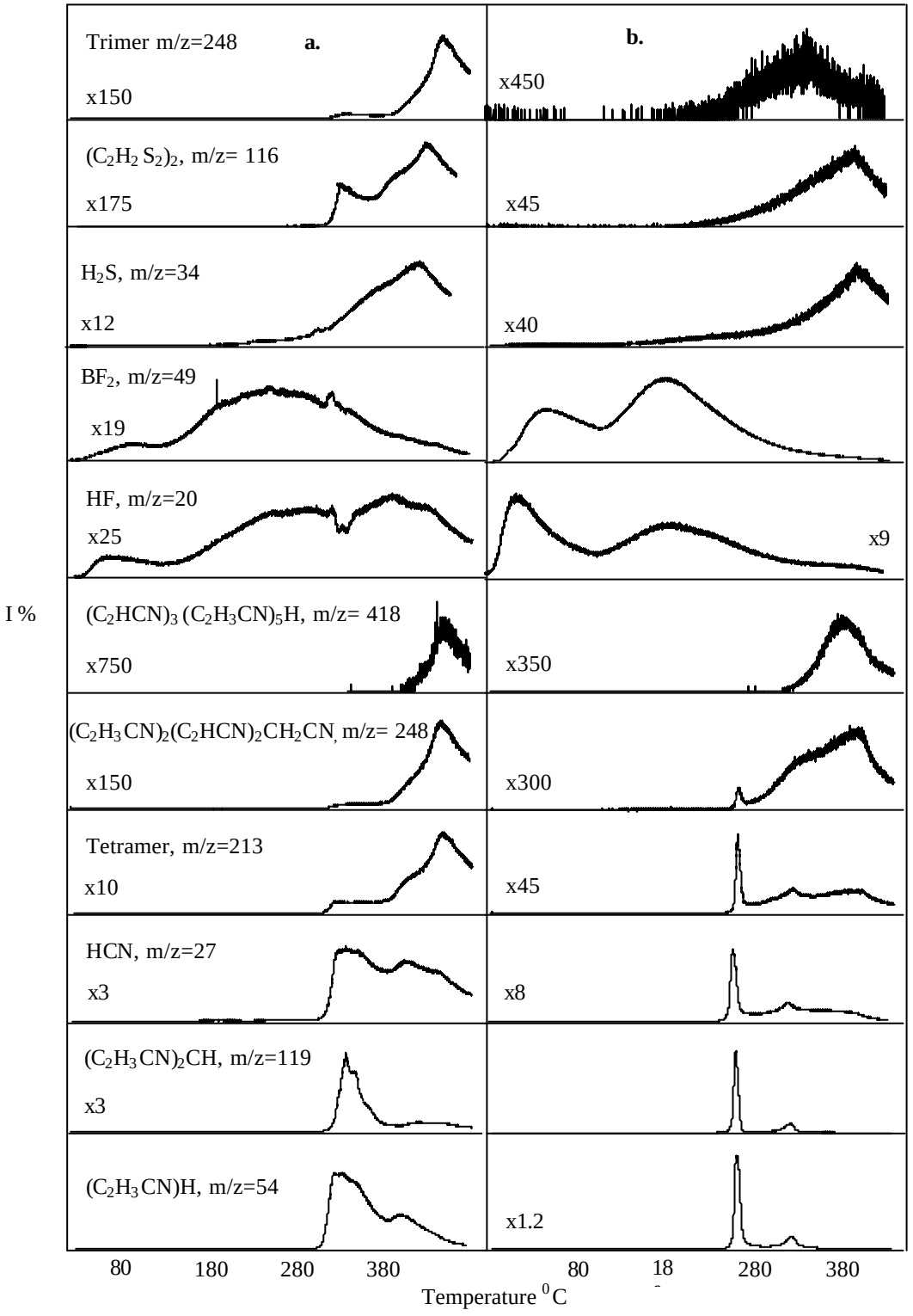

Figure III.16 The single ion pyrograms of some characteristic thermal decomposition products of a. polythiophene and polyacrylonitrile chains generated during the pyrolysis of PAN/PTh, b. corresponding homopolymers

The similarities in the evolution profiles of degradation products of the mechanical mixture and those of the corresponding homopolymers were quite significant. When the thermal decomposition products of PTh considered, the only difference detected was the decrease in the intensity of the low temperature evolution peak of dopant based products that were attributed to the physically adsorbed dopant and HF generated by reactions of dopant with adsorbed water [56]. The evolution profiles of PAN based products generated from PAN and the mechanical mixture showed nearly identical trends. The monomer and the low molecular weight oligomers of acrylonitrile and the fragments due to the homolytic cleavages along the polymer backbone were mainly generated in a narrow temperature range around 320 ^{0}C, whereas the fragments associated with relatively high molecular weight unsaturated cyclic imine structures were recorded at high temperatures and were quite weak. It is clear that each component degraded independently during the pyrolysis of the mechanical mixture.

On the other hand, evolution profiles of PAN based products recorded during pyrolysis of PTh/PAN films showed significant differences compared to those recorded for the pure homopolymer, PAN. In general, the evolution profiles of products generated by homolytic cleavages shifted slightly to higher temperatures and broadened, whereas the products due to the cleavages at the α-carbon diminished in intensity. Significant increase in HCN evolution at elevated temperatures was also detected. Furthermore, the relative intensities of high molecular weight fragments involving unsaturated cyclic structures increased considerably, especially in the final stages of pyrolysis. Some variations in the evolution profiles of PTh based products were also detected. Yet, the changes were almost negligible. Meanwhile, the relative intensities of dopant based fragments such as BF_3, BF_2, and BF were decreased significantly while HF generation was enhanced even at elevated temperatures. The decrease in the dopant yield may be associated with a decrease in the extent of doping. However, if this was the case then evolution of HF should also be decreased accordingly. In general, HF generation is attributed to reactions of dopant with adsorbed H_2O usually during storage as shown in the Section III.2.

Thus, evolution of HF mainly expected to occur at initial stages of pyrolysis. Detection of HF at elevated temperatures, especially in the regions where evolution of other dopant based products already diminished, was associated with fluorine substituted thiophene rings in our previous studies [56]. Thus it may be concluded that fluorination of the polymer matrix has occurred under the experimental conditions.

It is clear, that thermal characteristics, thus, structural characteristics of both PAN and PTh blocks were affected during the electrochemical polymerization of thiophene onto PAN coated anode. However, in order to propose a copolymer formation, fragments involving characteristic units of both components should be detected. Thus, the presence of such products namely mixed dimers C_2H_3CN-C_4H_2S, $(C_2H_3CN)_2$-C_4H_2S C_2H_3CN-$(C_4H_2S)_2$ $(C_2H_3CN)_2$-$(C_4H_2S)_2$ has been questioned. In Figure 17 single ion pyrograms of C_2H_3CN-C_4H_2S, $(C_2H_3CN)_2$-C_4H_2S C_2H_3CN-$(C_4H_2S)_2$ $(C_2H_3CN)_2$-$(C_4H_2S)_2$ (m/z = 135, 188, 217, and 270 Da respectively) recorded during the pyrolysis of PTh/PAN and the mechanical mixture are shown together. Evolution profiles for C_2H_3CNH and $(C_2H_3CN)_2$ are also included for comparison. It is clear that the fragments with structures $(C_2H_3)_5$, $(C_2H_3CN)(C_2H_3)_5$ (m/z= 135 and 188 Da respectively) due to loss of CN, $(C_2HCN)_4CH$ and $(C_2HCN)_4(C_2H_3CN)$ (m/z= 217 and 270 Da respectively) due to dehydrogenation of cyclic segments along the polymer chain were generated from the homopolymer, PAN also. However, the relative intensities of these peaks, especially the fragments with molecular weights of 217 and 270 Da were significantly increased unlike the other fragments involving similar structures such as $(C_2HCN)_3(C_2H_3CN)_5$ in the high temperature pyrolysis mass spectra of PTh/PAN sample. Taking also into account the enhancements of products due homolytic cleavages compared to ones attributed to presence of unsaturated cyclic imine structures for PTh/PAN sample, it may be proposed that the characteristic cyclization reactions for PAN were limited for the BF_4^- doped PTh/PAN sample. Thus, it may be proposed that copolymerization PTh and PAN has been achieved.

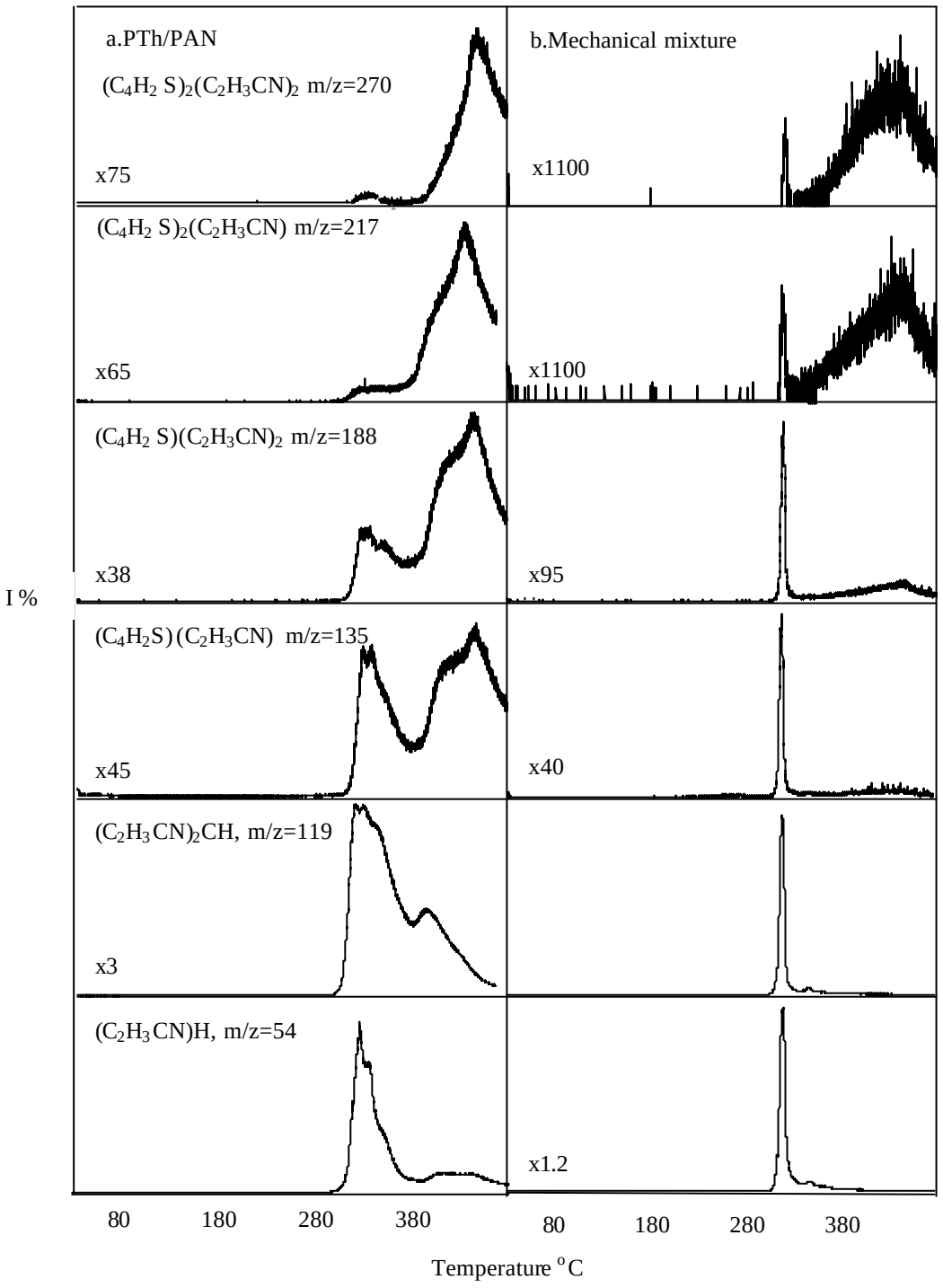

Figure III.17 Single ion pyrograms of C_2H_3CN-C_4H_2S, $(C_2H_3CN)_2$-C_4H_2 C_2H_3CN-$(C_4H_2S)_2$, $(C_2H_3CN)_2$-$(C_4H_2S)_2$ (m/z = 135, 188, 217, and 270 Da respectively) and C_2H_3CNH and $(C_2H_3CN)_2$ ((m/z = 54 and 119 Da, respectively) recorded during pyrolysis of PTh/PAN and b. the mechanical mixture

III.5. Copolymer of Polybutadiene and Polyacrylonitrile (PB/PAN)

In this section, the direct insertion probe pyrolysis mass spectrometry analyses of poly(acrylonitrile-co-butadiene)PB/PAN copolymer and mechanical mixture of PB and PAN were studied by application of direct pyrolysis mass spectrometry.

The total ion current (TIC) curve recorded during the pyrolysis of PB/PAN copolymer is shown in Figure III.18. together with the TIC curves for the mechanical mixture and the corresponding homopolymers PAN and PB. It is clear that the TIC curve of PB/PAN is significantly different than all of the others, whereas that of the mechanical mixture shows characteristic peaks of both components. The TIC curve of the copolymer shifted to higher temperatures indicating an increase in thermal stability. The pyrolysis mass spectra recorded at the maxima of the TIC curve of the copolymer are shown in Figure III.18. Although the TIC curve of the copolymer showed no resemblance to that of PAN and PB, peaks due to both components were detected in the pyrolysis mass spectra. Yet, the relative intensities were quite different. The base peak was at m/z=41 Da due to C_3H_5. Furthermore, the yield of low molecular weight fragments increased significantly. In Table III.6 the relative intensities of intense and/or characteristic peaks present in the pyrolysis mass spectra are summarized.

The evolution profiles of characteristic fragments from both components PAN and PB are given in Figures III.19 and III.20. Actually, as both components involve monomers with similar molecular weights, the pyrolysis mass spectra were dominated with peaks with similar m/z values. However, the thermal degradation mechanisms of PAN and PB are quite different. Thus, although identical peaks were detected in the mass spectra, evolution profiles were significantly different. It can be observed from Figures III.19 and III.20 that evolution profiles of the thermal degradation products of the copolymer were nearly identical. The low temperature peak in the TIC curve disappeared in the pyrograms of high molecular weight fragments as expected, as cleavage of high molecular fragments are enhanced at high temperatures. During the thermal degradation of a block copolymer, both components behave independently and a TIC curve similar to the TIC curve of a

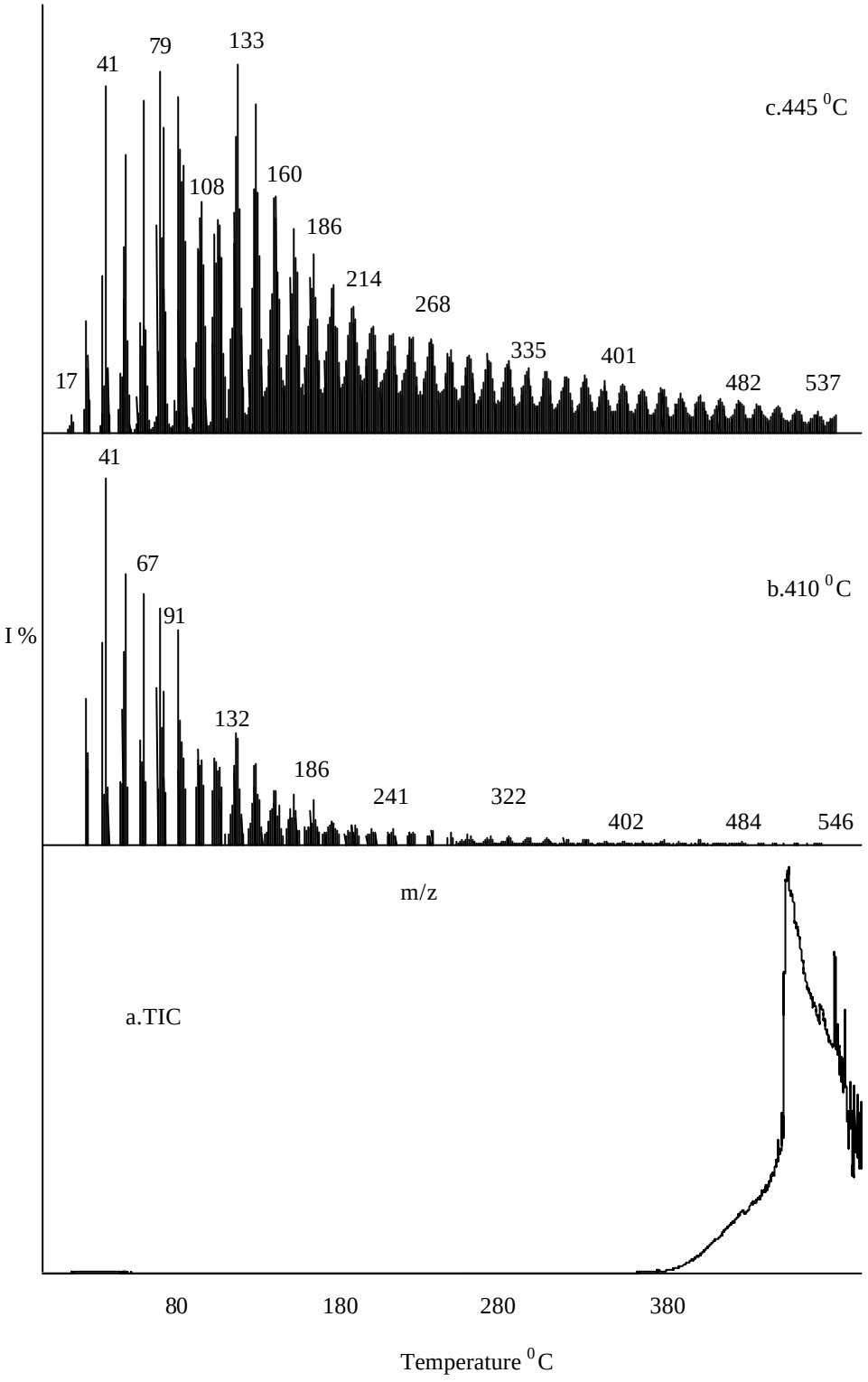

Figure III.18 a. TIC curve and the mass spectra recorded at b. 410 ^{0}C and c. 445 ^{0}C during the pyrolysis of PB/PAN

Table III.6. The intense and/or characteristics peaks recorded in the pyrolysis mass spectra recorded at the maxima of the TIC curves of PB/PAN

m/z	Relative Yield		Assignment
	410 ^{0}C	445 ^{0}C	
26	80	57	C_2H_2, CN
27	360	283	C_2H_3, HCN
28	230	153	C_2H_4, N_2
41	1000	918	C_3H_5
54	560	475	C_4H_6, $(C_2H_3CN)H$
57	70	94	C_4H_9
79	660	961	C_6H_7
119	240	560	$(C_2H_3CN)_2CH$
186	130	500	$(C_2H_3CN)_3C_2H_3$
255	48	257	$(C_4H_6)_4C_3H_3$
266	30	230	$(C_2H_3CN)_5$
324	28	120	$(C_4H_6)_6$
366		71	$(C_2HCN)_3$-$(C_2H_3CN)_4H$
377	20	134	$(C_4H_6)_5(C_2H_3CN)_2H$
417	10	99	$(C_4H_6)_7C_3H_3$
419		58	$(C_2HCN)_3$-$(C_2H_3CN)_5H$
431	10	95	$(C_4H_6)_7(C_2H_3CN)$
439	10	92	$(C_4H_6)_8(C_2H_3CN)_2H$
540		38	$(C_4H_6)_{10}$

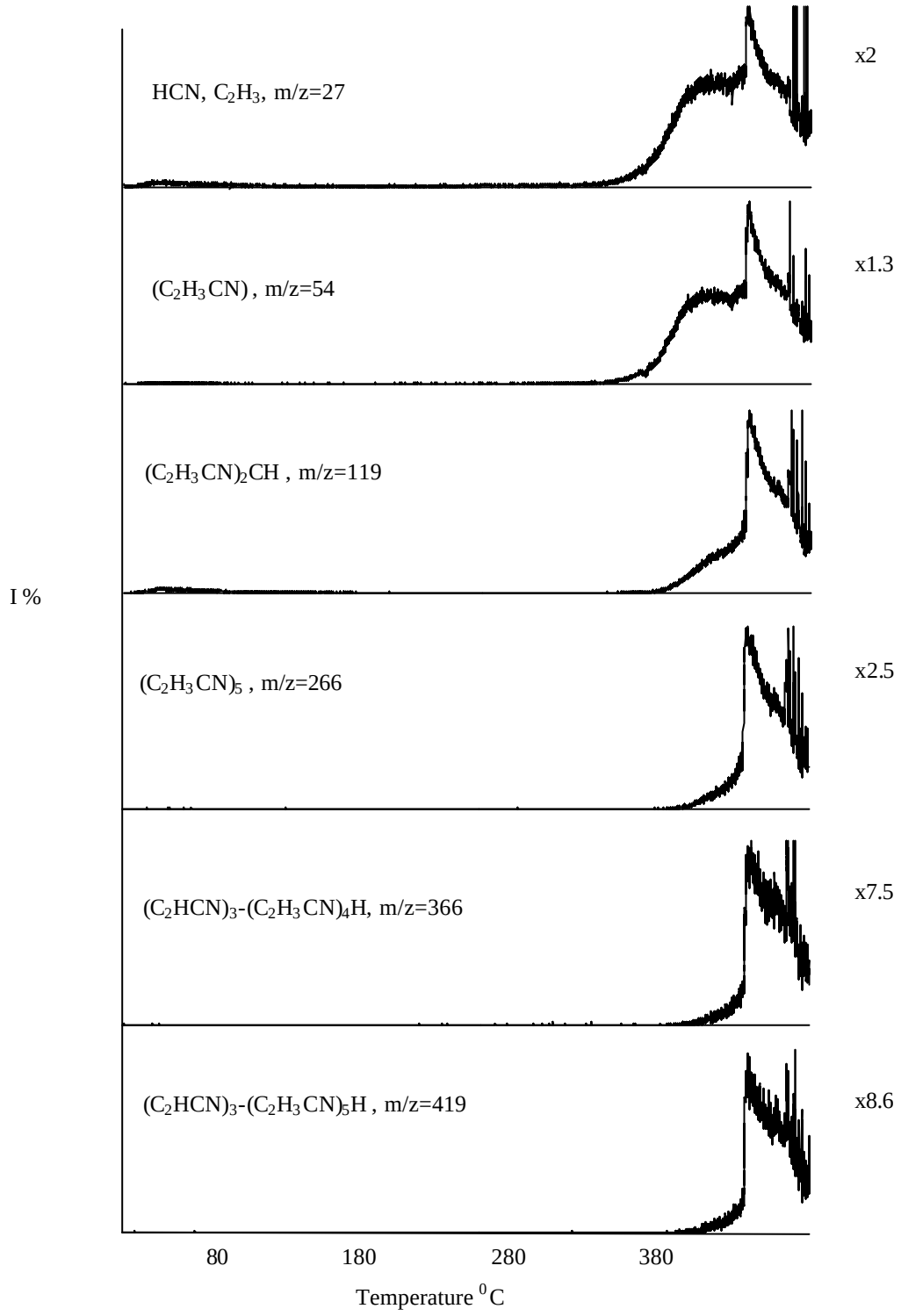

Figure III. 19 Single ion pyrograms of the ions, characteristic fragments from PAN, at m/z 27, 54, 119, 266, 366 and 419 Da recorded during the pyrolysis of PB/PAN

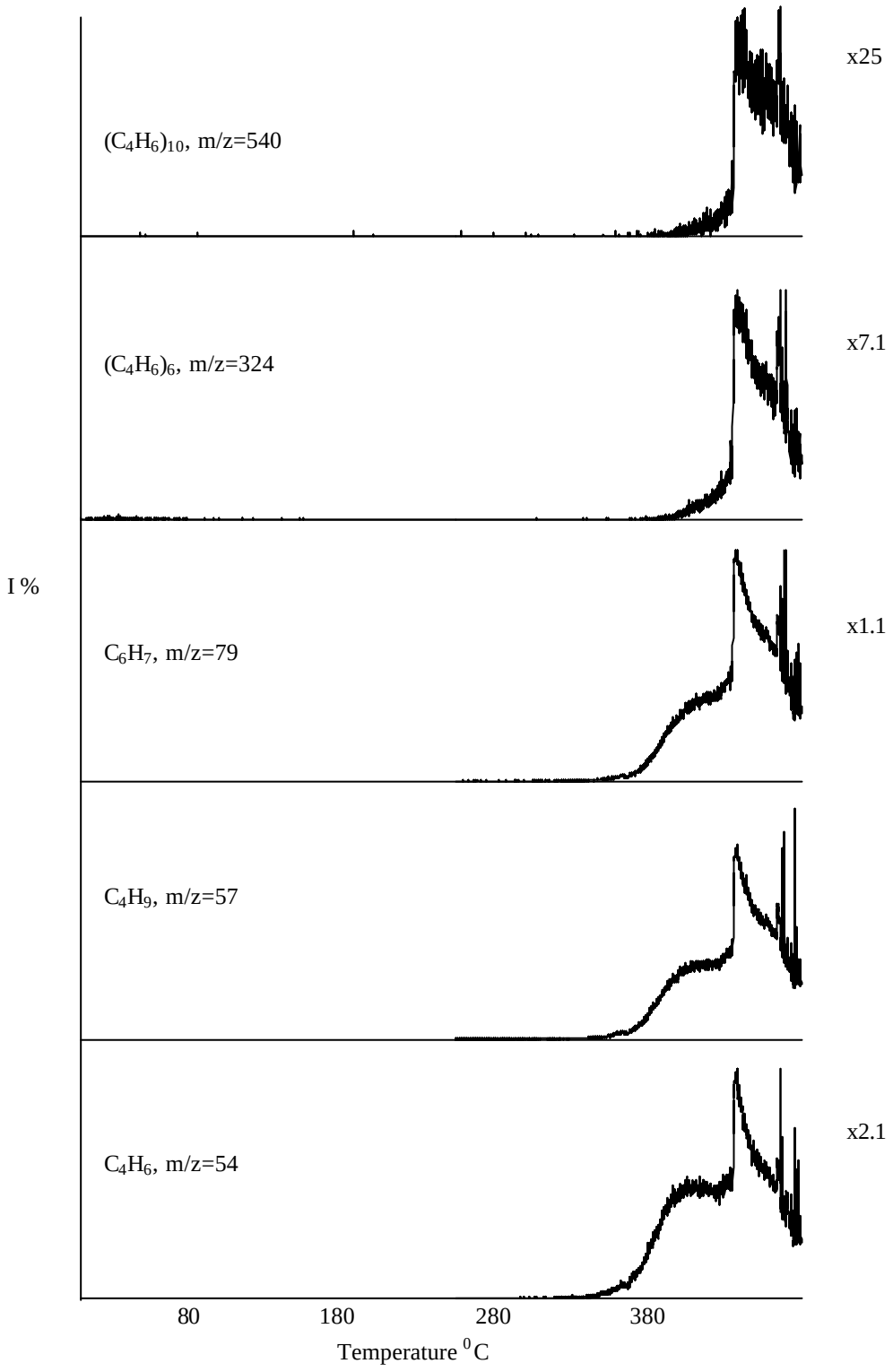

Figure III.20 Single ion pyrograms of the ions, characteristic fragments from PB, at m/z 54, 57, 79, 324 and 540 Da recorded during the pyrolysis of PB/PAN

mechanical mixture is detected. However, in general, the TIC curve of a random copolymer shows no resemblance to the TIC curves of both components and the mechanical mixture as detected for this case. Thus, the trends observed both in the TIC curve and the evolution profiles confirm presence of a random copolymer. The reactivity ratios of acrylonitrile and butadiene are 0.02 and 0.3 respectively indicating that the both monomers prefer to react with the other monomer. As the reactivity ratio of acrylonitrile is very low, the probability of finding long acrylonitrile segments is quite low. Thus, cyclization and crosslinking reactions detected for PAN are not likely during pyrolysis for the copolymer. On the other hand, the loss of cyano groups should be enhanced. The experimental data supports these general expectations. The relative intensities of peaks at m/z=26 Da due to C_2H_2, and CN, at m/z=27 Da due to C_2H_3 and HCN and at m/z=28 Da due to C_2H_4 and N_2 increased drastically. The low molecular fragment peaks were more intense in the pyrolysis mass spectra of PAN compared to PB. The intensity ratios of base peak at 54 Da to the peak at 27 and 26 Da were 7.2 and 18.6 respectively in the pyrolysis mass spectra of PAN, whereas, they were 11 and 60 for those of PB. For the copolymer the ratios increased to 1.6 and 6.7 indicating that cleavage of side groups were enhanced for the copolymer.

The total ion current curve of an aged poly(acrylonitrile-co-butadiene) copolymer at room temperature in air and in dark for a period of two years is given in Figure III.21. The presence of several peaks at low temperatures indicated presence of low molecular weight species in the sample. The pyrolysis mass spectra recorded at initial stages of pyrolysis indicated presence of monomer units of both components. Furthermore, the spectra are dominated with peaks that were not detected in those of the homopolymers and the copolymer. Spectral subtraction and comparison with library data indicated presence of oxygenated compounds such as $C_{25}H_{31}NO_2$ (Mwt= 377 Da), $C_{18}H_{34}O_2$ oleic acid and $C_{16}H_{32}O_2$ hexadecanoic acid. Evolution profiles of some of the differentiated products are shown in Figure III.22. Thus, it can be concluded that oxidative degradation of the copolymer occurs even if it is stored in dark and at room temperature.

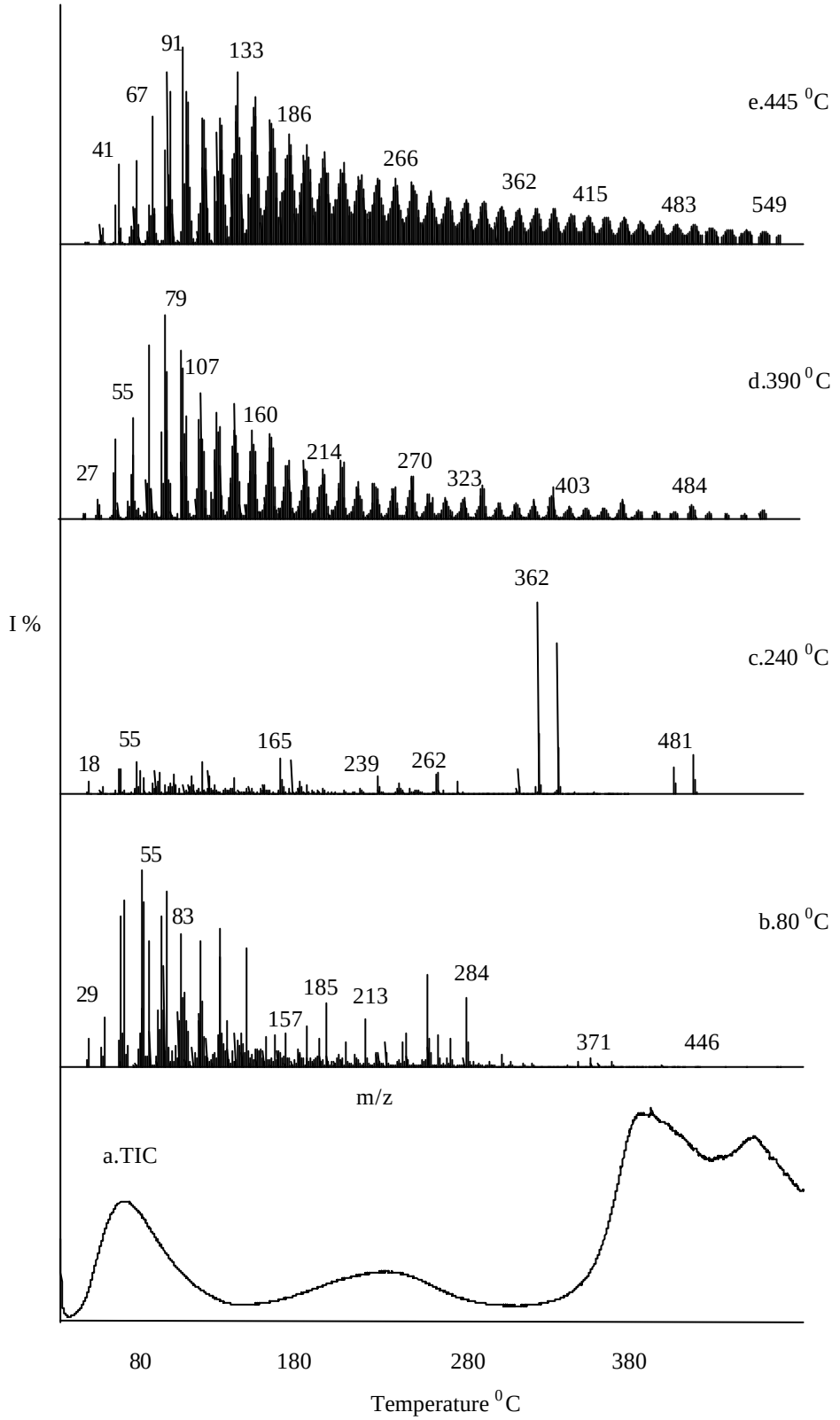

Figure III.21 a. The TIC curve and the mass spectra recorded at b. 80 ^{0}C, c. 240 ^{0}C, d. 390 ^{0}C and e. 445 ^{0}C during the pyrolysis of aged poly(acrylonitrile-co-butadiene) copolymer

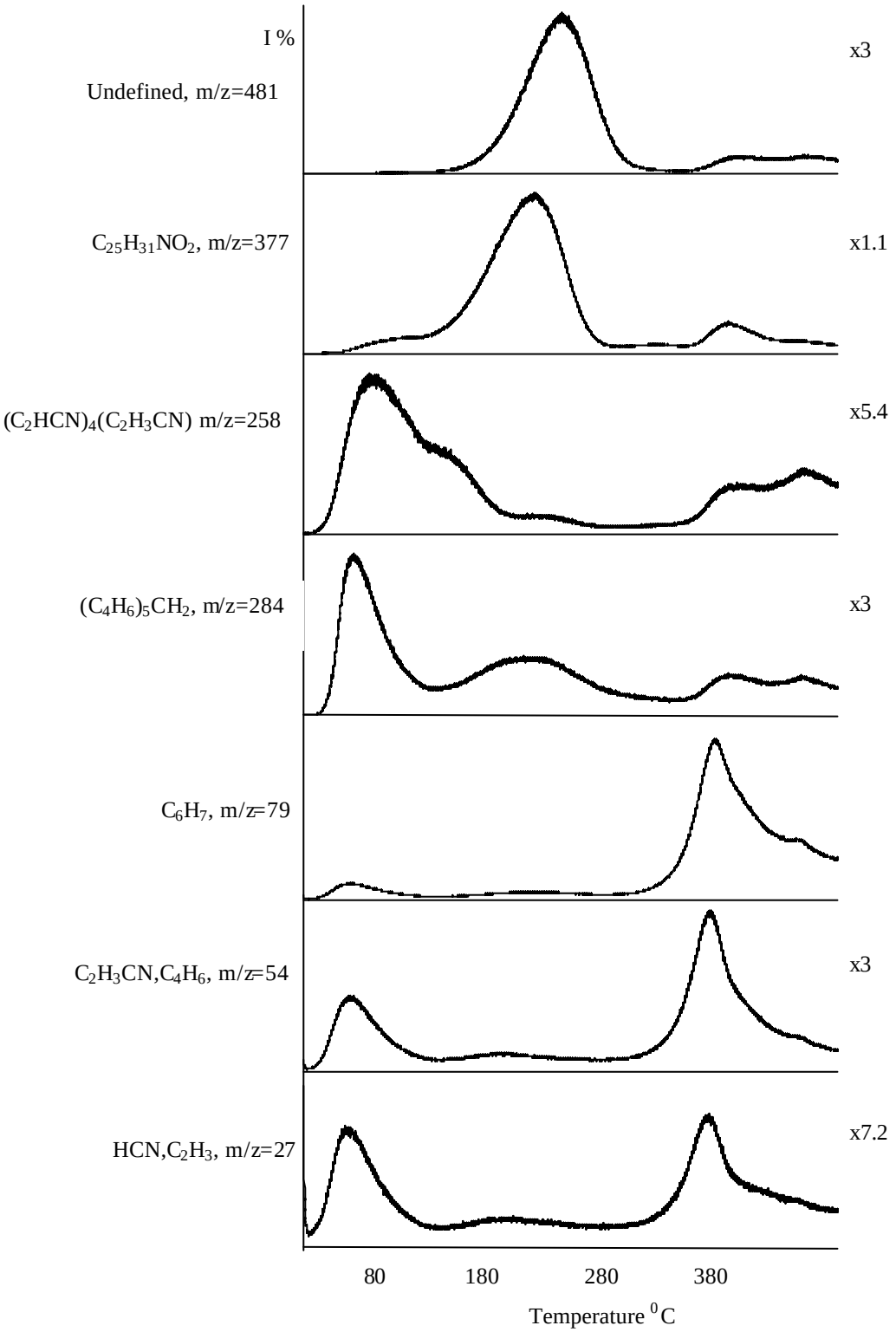

Figure III.22. Single ion pyrograms of the ions at m/z 27, 54, 79, 258, 284 and 481 Da recorded during the pyrolysis of aged poly(acrylonitrile-co-butadiene) copolymer

CHAPTER IV

CONCLUSIONS

In the first part of this study, the structural and thermal characteristics of a conducting polymer of polyacrylonitrile/polythiophene (PAN/PTh) have been studied by direct insertion probe pyrolysis mass spectrometry technique. The sample was prepared by electrochemical polymerization of thiophene on a polyacrylonitrile coated working electrode in acetonitrile/tetrabutylammoniumtetrafluoroborate solvent-electrolyte system. In order to get a better in sight, pyrolysis analyses of polyacrylonitrile (PAN), polyacrylonitrile films treated under the electrolysis conditions in the absence of thiophene, polythiophene, (PTh) and the mechanical mixture have also been performed. The following can be concluded in the light of present results.

- The thermal degradation of polyacrylonitrile occurs in three steps. In the first step, random chain cleavages were occurred along the polymer backbone and in the second decomposition step, crosslinked and unsaturated segments confirming dehydrogenation were observed. Evolution of HCN, monomer, low molecular weight oligomers and products stabilized by cyclization and dehydrogenation reactions were recorded around 300^0C. At elevated temperatures, the unsaturation along the polymer backbone was determined to be increased.

- When polyacrylonitrile films treated under the electrolysis conditions in the absence of thiophene were pyrolyzed, decrease in the yields of monomer and oligomers, and increase in the amount of products stabilized by cyclization reactions were detected.

- The thermal decomposition of polythiophene occurs in two steps. The first step corresponds to the loss of the dopant and the second step corresponds to the degradation of polymer backbone.

- The evolution profiles of PTh based products from PTh/PAN showed nearly identical trends with those recorded during the pyrolysis of pure PTh. However, when PAN based products were considered, contrary to the trends observed for pure PAN, evolution of HCN and the degradation products due to the homolytic cleavages of the polymer backbone continued through out the pyrolysis indicating a significant increase in their production even at the final stages of pyrolysis. On the other hand, the yield of thermal degradation products associated with decomposition of the unsaturated cyclic imine segments decreased. A careful analysis of the data pointed out presence of mixed dimers confirming copolymer formation.

In the second part of this study, fresh and aged poly(acrylonitrile-co-butadiene) samples that involve components with monomer units having quite similar molecular weights have been analyzed in order to investigate the limits of the pyrolysis mass spectrometry technique. The results lead to the following conclusions

- It has been shown that although, the two components can not be differentiated, the results can be used to determine changes in the thermal and structural characteristics compared to the corresponding homopolymers.

- The total ion current curve of the PB/PAN copolymer was significantly different than those of the corresponding homopolymers indicating presence of a random copolymer involving only short segments of each component.

- Pyrolysis of aged poly(acrylonitrile-co-butadiene) indicated oxidative degradation of the sample even in dark and room temperature conditions.

REFERENCES

1. P. Chandrasekhar, *Conducting Polymers, Fundamentals and Applications*, Kluwer Academic Publishers, USA, **1999**

2. J. Roncali, *Chem. Rev.*,92, **1992**, 711-738

3. H. Shirakawa, E. J. Louis, A. G. MacDiarmid, C. K.Chiang and A. J. Heeger, *J. Chem. Soc. Chem. Comm*, **1977**, 578-580

4. H. L. Wang, L. Toppare and J.E. Fernandez, *Macromolecules*, 26, **1990**, 1344

5. F. Selampinar, U. Akbulut, T. Yilmaz, A. Güngör and L. Toppare, *J. Appl. Polym. Sci.*, 35, **1997**, 3009

6. D. Stanke, M.L. Hallensleben and L. Toppare, *Synthetic Metals*, 72, **1995**, 167

7. D. Stanke, M.L. Hallensleben and L. Toppare, *Synthetic Metals*, 73, **1995**, 261

8. M. Kabasakaloglu, T. Kiyak, H. Toprak, M.L. Aksu, *Applied Surface Science*, 152, **1999**, 115-125

9. Y.Takenaka, T. Koike, T. Oka, M. Tanahashi, *Synthetic Metals*, 18, **1987**, 207-212

10. G. Tourillon, F. Garnier, *J.Electroanal. Chem.*, 135, **1982**, 173-176

11. H. Tang, L. Zhu, Y. Harima, K. Yamashita, *Synthetic Metals*, 110, **2000**, 105-113

12. G. Tourillon, F. Garnier, *J.Phys. Chem.*, 87, **1983**, 2289-2292

13. K. Gurunathan, A.V. Murugan, R. Marimuthu, U.P. Mulik, D.P. Amelnerkar, *Materials Chemistry and Physics*, 61, **1999**, 173-191

14. C. K. Chiang, S.C. Gau, C.R. Fincher, Y.W. Park, A.G. MacDiarmid, A.J. Heeger, *App. Phys. Lett.*, 33(1), **1978**, 18-20

15. B. Ballarin, R. Seeber, D. Tonelli, F. Andreani, P.C. Bizzarri, C.D. Casa, E. Salatelli, *Synthetic Metals*, 88, **1997**, 7-13

16. Y.H. Park, M.H. Han, *Journal of Applied Polymer Science*, 45, **1992**, 1973-1982

17. K. Imanishi, M. Satoh, Y. Yasuda, R. Tsushima, S. Aoki, *J.Electroanal. Chem.*, 242, **1988**, 203-208

18. D. Singh, S. Dubey, M. Prasad, R.A. Misra, *Journal of Applied polymer Science*, 73, **1999**, 91-98

19. A.J. Downard and D. Pletcher, *J. Electroanal. Chem.*, 206, **1986**, 147-152

20. G.B. Street, T.C. Clarke, M. Kroumbi, K. Kanazawa, V. Lee, P. Pfluger, J.C. Scott and G. Weiser, *Mol. Cryst. Liq. Cryst*., 83, **1982**, 253-260

21. J.E. Österholm, P. Sunila and T. Hjertberg, *Synthetic Metals*, 18, **1987**, 169-176

22. B. Wehrle, H.H. Limbach, J. Mortensen, J. Heinze, *Synthetic Metals*, 38, **1990**, 293-301

23. H. Kato, D. Nishikawa, T. Matsui, S. Honma, H. Kokado, *J. Phys. Chem*., 95, **1991**, 6014-6022

24. T.C Clarke, J.C. Scott, G.B. Stree, *J. Res. Dev*., 27, **1983**, 313-320

25. B.K. Moss and R.P. Burford, *Polymer International*, 26, **1991**, 225-230

26. T. Gozet, A.M.Onal, J. Hacaloglu, *Synthetic Metals*, 135-136, **2003**, 453-454

27. Y. Cao, P. Wang and R. Quian, *Macromol. Chem*., 186, *1985*, 1093,1102

28. E. Ando, S. Onodera, M. Iino and O. Ito, *Carbon*, 39, *2001*, 101-108

29. F. Mohammad, P.D. Calvert, N.C. Billingham, *Synthetic Metals*, 66, **1994**, 33-41

30. S. Yigit, J. Hacaloglu, U. Akbulut, L. Toppare, *Synthetic Metals*, 84, **1997**, 205-206

31. E. Kalaycioglu, L. Toppare, Y. Yagci, V. Harabagiu, M. Pintela, R. Ardelean, B.C. Simionescu, *Synthetic Metals*, 97, **1998**, 7-12

32. J. Hacaloglu, S. Yigit, U. Akbulut, L. Toppare, *Polymer*, 38, **1997**, 5119-5124

33. T. Uyar, L. Toppare, J. Hacaloglu, *J. Anal. Appl. Pyrolysis*, 68-69, **2003**, 15-24

34. B. François, T. Olinga, *Synthetic Metals*, 55-57, **1993**, 3489-3494

35. E. Kalaycioglu, L. Toppare, Y. Yagci, *Synthetic Metals*, 108, **2000**, 1-7

36. S. Öztemiz, L. Toppare, A. Önen, Y. Yagci, *J.M.S.-Pure Appl. Chem*., A37(3), **2000**, 277-291

37. P. Yildirim, Z. Küçükyavuz, *Synthetic Metals*, 95, **1998**, 17-22

38. S. Yigit, J. Hacaloglu, U. Akbulut and L. Toppare, *Synthetic Metals*, 84, **1997**, 205-206

39. Luis Geraldo Cardoso dos Santos and Yoshio Kawano, *Polymer Degradation and Stability*, 44, **1994**, 27-32

40. T.J. Xue, M.A. McKinney and C. A. Wilkie, *Polymer Degradation and Stability*, 58, **1997**, 193-202

41. M. Surianarayanan, T. Uchida, M. Wakakura, *Journal of Loss Prevention in the Process Industries*, 11, **1998**, 99-108

42. G. Mengoli, C. Pagura, R. Salmaso, R. Tomat and S. Zecchin, *Synthetic Metals*, 16, **1986**, 173-188

43. S. Leroy, C. Boiziau, J. Perreau, C. Reynaud, G. Zalczer, G. Lecayon and C. Le Gressus, *Journal of Molecular Structure*, 128, **1985**, 269-281

44. F. Chen, J. Qian, *Fuel Processing Technology*, 67, **2000**, 53-60

45. D.D. Jiang, G.F. Levchik, S. V. Levchik, C.A. Wilkie, *Polymer Degradation and Stability*, 65, **1999**, 387-394

46. Sung-Seen Choi, *Journal of Analytical and Applied Pyrolysis*, 57, **2001**, 249-259

47. A. Ghassempour, N.M. Najafi, A.A. Amiri, *J. Anal. Appl. Pyrolysis*, 70, **2003**, 251-261

48. B.S. Radovic, R. Goodacre, E. Anklam, *J. Anal. Appl. Pyrolysis*, 60, **2001**, 79-87)

49. H. Fazlioglu, J. Hacaloglu, *J. Anal. Appl. Pyrolysis*, 63, **2002**, 327-338

50. T. Gozet, A.M. Onal, J. Hacaloglu, *Synthetic Metals*, 135-136, **2003**, 453-454

51. J. Hacaloglu, M.M. Fares, S. Süzer, *European Polymer Journal*, 35, **1999**, 939-944

52. T. Uyar, L. Toppare, J. Hacaloglu, *Synthetic Metals*, 123, **2001**, 335-342

53. S.M. Badawy, *Radiation Physics and Chemistry*, 61, **2001**, 143-148

54. T. Uyar, L. Toppare and J. Hacaloglu, *Synthetic Metals*, 119, **2001**, 307-308

55. Fried Joel R., *Polymer Science and Technology*, 2nd edition

56. F.Mohammad, *J.Phys. D:Appl. Phys*., 31, **1998**, 951